© 2018. Published by The Company of Biologists Ltd | Development (2018) 145, dev161158. doi:10.1242/dev.161158

STEM CELLS AND REGENERATION

RESEARCH ARTICLE

A regulatory pathway involving retinoic acid and calcineurin demarcates and maintains joint cells and osteoblasts in regenerating fin

Stephanie C. McMillan[1,2,*], Jing Zhang[2,3,*], Hue-Eileen Phan[2,3], Shirine Jeradi[4,5], Leona Probst[2,3], Matthias Hammerschmidt[4] and Marie-Andrée Akimenko[2,3,‡]

ABSTRACT

During zebrafish fin regeneration, blastema cells lining the epidermis differentiate into osteoblasts and joint cells to reconstruct the segmented bony rays. We show that osteoblasts and joint cells originate from a common cell lineage, but are committed to different cell fates. Pre-osteoblasts expressing *runx2a/b* commit to the osteoblast lineage upon expressing *sp7*, whereas the strong upregulation of *hoxa13a* correlates with a commitment to a joint cell type. In the distal regenerate, *hoxa13a*, *evx1* and *pthlha* are sequentially upregulated at regular intervals to define the newly identified presumptive joint cells. Presumptive joint cells mature into joint-forming cells, a distinct cell cluster that maintains the expression of these factors. Analysis of *evx1* null mutants reveals that *evx1* is acting upstream of *pthlha* and downstream of or in parallel with *hoxa13a*. Calcineurin activity, potentially through the inhibition of retinoic acid signaling, regulates *evx1*, *pthlha* and *hoxa13a* expression during joint formation. Furthermore, retinoic acid treatment induces osteoblast differentiation in mature joint cells, leading to ectopic bone deposition in joint regions. Overall, our data reveal a novel regulatory pathway essential for joint formation in the regenerating fin.

KEY WORDS: Joints, Osteoblasts, Zebrafish fin regeneration, *hoxa13a*, *pthlha*, *evx1*

INTRODUCTION

During zebrafish fin regeneration, lineage-restricted cells proximal to the amputation site migrate distally, proliferate, and de-differentiate to form the blastema underneath the newly formed wound epidermis (Knopf et al., 2011; Nechiporuk and Keating, 2002; Poleo et al., 2001; Poss et al., 2003; Santos-Ruiz et al., 2002; Tu and Johnson, 2011). Subsequently, cells leave the blastema and enter the differentiation zone where they differentiate into the multiple cell types that reform the lost fin (Borday et al., 2001; Knopf et al., 2011; Tu and Johnson, 2011). Blastema cells that enter the differentiation zone and come into contact with basal epidermal cells differentiate into osteoblasts expressing *indian hedgehog a* (*ihha*) and *patched 2* (*ptch2*) [previously called *patched 1* (*ptch1*)] (Avaron et al., 2006; Borday et al., 2001; Gavaia et al., 2006; Knopf et al., 2011; Laforest et al., 1998; Sousa et al., 2011). Previously, it was shown that *bone morphogenetic protein 2b*, a downstream target of Hedgehog signaling, mediates osteoblast differentiation through induction of the early osteoblast markers *runt-related transcription factor 2a* and *2b* (*runx2a* and *runx2b*) (Nakashima et al., 2002; Smith et al., 2006). Upon commitment to an osteoblast cell fate, cells express *sp7* (also named *osterix*, *osx*), and further differentiation results in the expression of the bone matrix genes *osteocalcin* [*osc*; also known as *bone gamma-carboxyglutamate* (*gla*) *protein* (*bglap*)] and *collagen*, *type X*, *alpha 1a* (*col10a1a*) (Avaron et al., 2006; Gavaia et al., 2006; Laforest et al., 1998; Sousa et al., 2011). These mature osteoblasts synthesize and release bone matrix into the subepidermal space to form the intramembranous bone of the fin rays (Akimenko et al., 2003; Becerra et al., 1996; Mari-Beffa et al., 1996; Santamaría et al., 1996). Furthermore, osteoblasts are periodically separated into segments by cells that ultimately form the fin ray joints.

Although the mechanisms controlling joint formation are unknown, joint regions express a unique set of genes that are involved in joint formation. The *even-skipped homeobox 1* (*evx1*) gene, expressed at the level of the joints, is required for joint formation as null mutants lack joints (Borday et al., 2001; Schulte et al., 2011; Sims et al., 2009). Currently, the mechanism by which Evx1 controls joint formation is unknown. However, mutations in *cx43* (*short fin*, sof^{b123}) and *kcnk5b* (*another long fin*, alf^{dty86}) alter *evx1* expression, resulting in shorter and longer/inconsistent fin ray segments, respectively (Sims et al., 2009). Furthermore, the sof^{b123} mutants possess short fin lengths (Hoptak-Solga et al., 2008; Iovine et al., 2005; Ton and Iovine, 2013), whereas the alf^{dty86} mutant possesses increased fin lengths (Hoptak-Solga et al., 2008; Perathoner et al., 2014; Ton and Iovine, 2013). Overall, there is a correlation between fin and segment length in the *sof* and *alf* mutants, indicating that the mechanisms controlling fin growth and joint formation may be linked. However, the *long fin* and *rapunzel* mutants possess long fins, but unaltered segment lengths (Goldsmith et al., 2003; Iovine and Johnson, 2000). Furthermore, $evx1^{i232}$ homozygous mutants have normal fin lengths (Schulte et al., 2011). These results indicate that growth and joint formation may also occur via independent processes.

Calcineurin, a Ser/Thr phosphatase (Klee and Haiech, 1980), was identified as a regulator of proportional growth control (isometric versus allometric) in zebrafish (Kujawski et al., 2014). Currently, the exact mechanism by which calcineurin regulates these processes is unknown. However, it has been suggested that calcineurin acts

[1]Department of Cellular and Molecular Medicine, University of Ottawa, Ottawa, ON, Canada K1N 6N5. [2]CAREG, 30 Marie Curie, University of Ottawa, Ottawa, ON, Canada K1N 6N5. [3]Department of Biology, 30 Marie Curie, University of Ottawa, Ottawa, ON, Canada K1N 6N5. [4]Institute for Developmental Biology, Cologne University, Cologne 50674, Germany. [5]Institut Polytechnique Privé, Université Libre de Tunis, Tunis 1003, Tunisia.
*These authors contributed equally to this work

‡Author for correspondence (makimen@uottawa.ca)

S.C.M., 0000-0003-0410-1338; J.Z., 0000-0002-7105-2292; S.J., 0000-0001-6412-7076; L.P., 0000-0001-6226-1060; M.-A.A., 0000-0002-1905-7731

Received 7 November 2017; Accepted 1 May 2018

Development (2018) 145, dev161158. doi:10.1242/dev.161158

upstream of retinoic acid (RA) signaling, another potential regulator of proximal-distal patterning (Kujawski et al., 2014). Considering the correlation between growth and joint formation, it is of interest to investigate whether calcineurin and retinoic acid play a role in joint formation. The addition of calcineurin and RA signaling data to existing mathematical models may clarify the mechanisms underlying growth and joint patterning in the fin regenerate (Rolland-Lagan et al., 2012).

In this study, we have analyzed joint cells along the proximal distal axis of the fin regenerate. Gene expression analysis indicates that osteoblasts and joint cells originate from a common cell lineage but are later committed to different cell fates. Based on gene expression analysis and changes in cell morphology, joint cell formation is divided into at least three stages: presumptive joint cells, joint-forming cells and mature joint cells. In presumptive joint cells, *evx1* is acting downstream of or in parallel with *homeobox A13a* (*hoxa13a*), but upstream of *parathyroid hormone-like hormone a* (*pthlha*). As joint cells mature, expression of *hoxa13a*, *evx1* and *pthlha* is maintained. However, treatment with a calcineurin inhibitor or RA inhibits expression of these three genes. This inhibition is accompanied by the differentiation of mature joint cells into osteoblasts and ectopic bone deposition into joint spaces. These data suggest that RA levels must be tightly controlled to form and maintain joints of the fin regenerate.

RESULTS

During development and regeneration, fin ray segmentation is established by the periodic distal addition of joints, forming new bone segments (Fig. 1A,A′) (Iovine and Johnson, 2000; Johnson and Bennett, 1998; Smith et al., 2006). The segments have a concave shape (Fig. S1A, Movie 1), and each segment is connected by collagenous ligaments (Fig. S1B). Although segment length progressively decreases along the adult caudal fin rays (Rolland-Lagan et al., 2012), the first two joints that were formed following a standard amputation were consistently separated by 237±34 µm (mean±s.d.; n=25). Using the last-formed joint as a reference, 4′,6-diamidino-2-phenylindole (DAPI) staining of longitudinal cryosections of 4 days post-amputation (dpa) fin regenerates revealed a small cell cluster aligned with osteoblasts 254±25 µm distal from the last-formed joint (n=12) (Fig. 1B,B′). Considering the distance similarity, we suggest that the cell cluster is located at the level of the newest forming joint observed on whole-mount fins (Fig. 1A,A′). This cell cluster corresponds to joint cells previously described by Sims et al. (2009). Therefore, the cell cluster will be termed ‘joint-forming cells’. Note that the cell cluster protrudes toward the basement membrane, leading to an indent in the basal epidermal layer (Fig. 1B,C-C″).

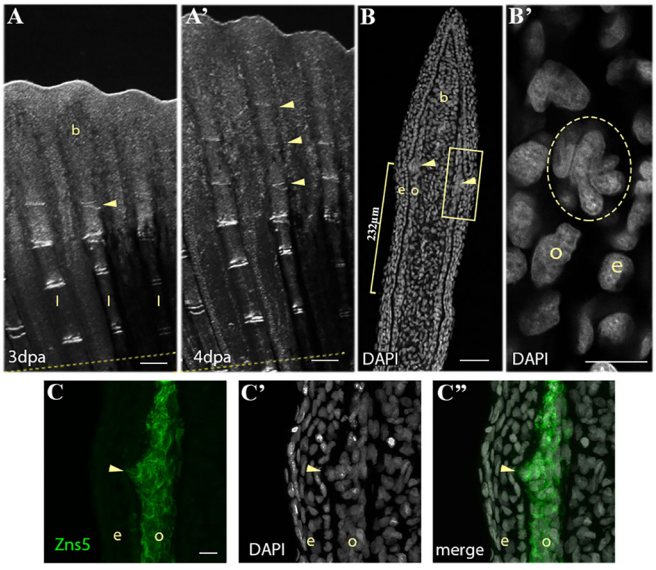

Fig. 1. Periodic formation of a cluster of joint-forming cells during fin regeneration. (A-A′) Bright-field images of fin regenerate at 3 dpa (A) and 4 dpa (A′) illustrate the periodic addition of joints (yellow arrowheads) to the distal end of the rays. Dashed yellow line indicates amputation plane. (B) DAPI staining on a 4 dpa regenerate longitudinal cryosection illustrates a cluster of nuclei (yellow arrowheads) 232 µm (yellow bracket) from a mature joint. (B′) Magnification of the boxed area in B showing the nuclei cluster (yellow circle). (C) Zns5 immunohistostaining labels the joint cell cluster and adjacent osteoblasts. (C′) DAPI staining of the same section showing the cell cluster nuclei. (C″) Merged image of C and C′. b, blastema; e, epidermis; l, lepidotrichia; o, osteoblast. Scale bars: 200 µm (A,A′); 50 µm (B); 10 µm (B′; in C for C-C″).

Zns5-positive joint cells express only early osteoblast differentiation markers

Because joint-forming cells align with differentiating osteoblasts, we investigated the relationship between joint cells and the osteoblast lineage. Zns5, an antibody that acts as a pan-osteoblast marker (Johnson and Weston, 1995), uniformly labeled joint-cell clusters and adjacent osteoblasts in the fin regenerate (Fig. 1C-C″). These results indicate that the joint-forming cells are of the osteoblast lineage. Gene expression analysis of osteoblast differentiation markers at 4 dpa revealed that *runx2a* and *runx2b* are expressed in osteoblasts and in a group of cells that appears as a ‘bump’, which likely corresponds to the joint-forming cells (Fig. 2A,B). Although surrounded medially by osteoblasts, joint-forming cells did not express *sp7* or *col10a1a*, as there is a gap in expression at the aforementioned ‘bump’ (Fig. 2C,D). At 4 dpa, *bglap* expression was restricted to the mature osteoblasts of the stump and proximal fin regenerate and was not expressed in joint-forming cells (Fig. 2E, Fig. S1C-C″). Reporter expression of the transgenic line *Tg(bglap:mCherry)* at 4 dpa confirmed that *bglap* is expressed in mature osteoblasts and is absent from joint regions (Fig. 2E′, Fig. S1D-D″). Overall, these data indicate that joint cells and osteoblasts originate from a common cell lineage, but joint cells do not continue down the osteoblast differentiation pathway.

Joint cells express *pthlha* but not *ihha*

Previously it has been shown that *ihha* is expressed in differentiating osteoblasts (Armstrong et al., 2017; Avaron et al., 2006). We further characterized *ihha* expression in relation to joint formation in the fin regenerate. In 10/23 sections of 4 dpa regenerates lacking joint-forming cells, *ihha* was expressed uniformly in differentiating osteoblasts, in agreement with Armstrong et al. (2017) and Avaron et al. (2006). However, when a ‘bump’ corresponding to the joint-forming cells was present (13/23 sections), there was a gap in *ihha* expression (Fig. 2F,F′). The reason for the presence or absence of the gap in *ihha* is likely to be related to the cyclical nature with which joints form in the regenerate. Therefore, similar to *sp7* and *col10a1a*, *ihha* was not detected by *in situ* hybridization (ISH) in joint-forming cells.

In mouse and chick, endochondral bone growth and differentiation are regulated by an Ihh/parathyroid hormone related protein (PTHrP) negative-feedback loop. Pre-hypertrophic chondrocytes leaving the proliferative pool express Ihh, which promotes PTHrP expression in perichondral cells and early proliferating chondrocytes. PTHrP signaling from these cells then

Development (2018) 145, dev161158. doi:10.1242/dev.161158

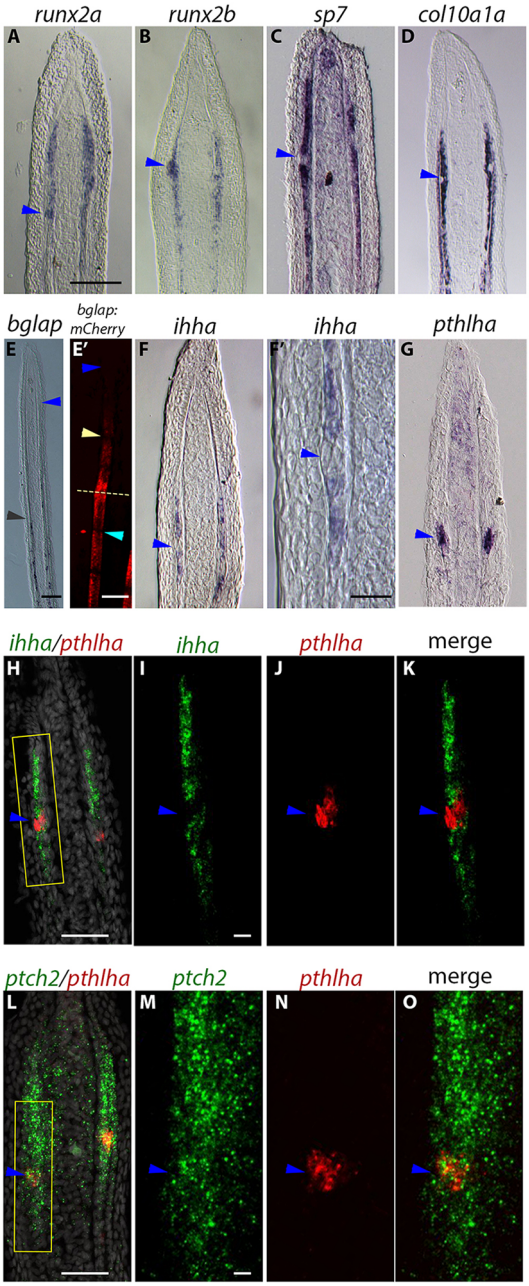

Fig. 2. Joint cells and osteoblasts originate from a common cell lineage, but are later committed to different cell fates. All panels show ISH and FISH data for various markers on longitudinal cryosections of 4 dpa fin regenerates except E′, which shows mCherry reporter expression. (A,B) *runx2a* and *runx2b* expression domains form a 'bump' at the joint-forming cell cluster (blue arrowheads). (C,D) Absence of *sp7* (C) and *col10a1a* (D) expression in the joint cell cluster (blue arrowheads). (E) The distal limit of the domain of expression of the late osteoblast marker *bglap* (black arrowhead) is proximal to the location of the joint-forming cells (approximate location indicated by blue arrowhead). (E′) mCherry reporter expression in *Tg(bglap:mCherry)* fish is absent in the distal regenerate (dark blue arrowhead), joints of the regenerate (yellow arrowhead), and mature joints in the stump (light blue arrowhead). Dashed line indicates the amputation plane. (F,F′) *ihha* is not expressed in the joint-forming cells (blue arrowheads). (G) In contrast, *pthlha* is expressed in the joint-forming cells (blue arrowhead). (H-O) Double FISH confirms *pthlha* expression in joint-forming cell clusters (blue arrowheads) that do not express *ihha* but do express *ptch2* (blue arrowheads). I, J and K show magnifications of the boxed area in H. M, N and O show magnifications of the boxed area in L. Scale bars: 100 µm (E; in A for A-D,F,G); 200 µm (E′); 10 µm (F′; in I for I-K; in M for M-O); 50 µm (H,L).

inhibits Ihh expression to promote chondrocyte proliferation and inhibit differentiation (Lanske et al., 1996; St-Jacques et al., 1999; Vortkamp et al., 1998). As a first step to investigate whether a similar interaction might occur in zebrafish fin regenerates, we analyzed *pthlha* expression, an ortholog of mammalian PTHrP (Yan et al., 2012). ISH on sections of 4 dpa fin regenerates indicated that *pthlha* is expressed in the blastema and strongly expressed in joint-forming cell clusters (Fig. 2G) and mature joints (Fig. 3A). Double fluorescence ISH (FISH) experiments confirmed *pthlha* expression in joint cells, and *ihha* expression only in osteoblasts (Fig. 2H-K, Fig. S2A-A″). However, *ptch2*, an Ihha receptor, was expressed in joint cells (Fig. 2L-O, Fig. S2B-B″). Expression of *ptch2* suggests that joint cells have the potential to respond to Ihha, secreted by surrounding osteoblasts.

We examined the expression of other Parathyroid hormone-like hormone (Pthlh) and Pthlh receptor genes. In zebrafish, there are two Pthlh (*pthlha* and *pthlhb*) and three Pthrp receptor (*pth1ra*, *pth2r* and *pth1rb*) genes originating from the teleost genome duplication (Yan et al., 2012). Non-quantitative RT-PCR revealed *pthlhb*, *pth1ra* and *pth2r*, but not *pth1rb*, expression in 4 dpa fin regenerates (Fig. S2C). ISH showed *pth1ra* expression in osteoblasts without gaps in expression (11/11 sections) indicating that *pth1ra* is expressed in joint-forming cells (Fig. S2D). No staining was observed for *pthlhb* and *pth2r* (data not shown), indicating that the expression levels are too low to be detected by ISH. Overall, these data indicate that *ihha* and *pthlha* possess complementary expression patterns that are reminiscent of those observed during endochondral and intramembranous ossification in other systems (Abzhanov et al., 2007; Lanske et al., 1996; St-Jacques et al., 1999; Vortkamp et al., 1998). Similar expression patterns indicate that Ihha and Pthlha may also interact during segment formation in zebrafish.

Characterization of a domain of presumptive joint cells

As rays grow via the distal addition of segments, joints present a distal-to-proximal gradient of maturation. ISH on whole-mount and longitudinal sections of 4 dpa regenerates revealed *pthlha* expression in joint cells at all maturation stages (Fig. 3A-A″). Additionally, a novel *pthlha* expression domain was observed in the distal-most pre-osteoblasts (Fig. 3A″, Fig. 4B′,C′). The distal *pthlha* domain was elongated compared with joint-forming cells (Figs 3 and 4), and was located 219±51 µm (n=24) distal to the joint-forming cells (Fig. 3A″). These data suggest that the distal *pthlha*-expressing cells are new joint cells that we will term 'presumptive joint cells'. Similarly, *evx1* was expressed in all joint cells, including the presumptive joint cells (Fig. 3B-B″). The *evx1* and *hoxa13a* genes are in close genomic proximity and possess similar expression patterns during pectoral fin development (Ahn and Ho, 2008). Furthermore, the *Tg(m-Inta11:eGFP)* transgene, which recapitulates embryonic *hoxa13a* expression (Kherdjemil et al., 2016), is expressed in joint cells (see below for more details). Therefore, *hoxa13a* expression was examined during fin regeneration. Similar to *pthlha* and *evx1*, *hoxa13a* was expressed in all joint cells including the presumptive joint cells (Fig. 3C-C″). *pthlha* and *hoxa13a* are also expressed in the blastema; however, only *hoxa13a* is faintly expressed in pre-osteoblasts and newly committed osteoblasts (Fig. 3A-A″,C′,C″). It is possible that *evx1* and *pthlha* may be expressed in osteoblasts at a low level that was undetectable by ISH. Other Hox genes (*hoxa11a*, *hoxa11b*, *hoxa13b* and *hoxd13a*) did not show expression in joint regions of 4 dpa regenerates by ISH (Fig. S2E-I).

Osteoblast marker expression was examined in the presence and absence of presumptive joint cells. In the absence of presumptive

Development (2018) 145, dev161158. doi:10.1242/dev.161158

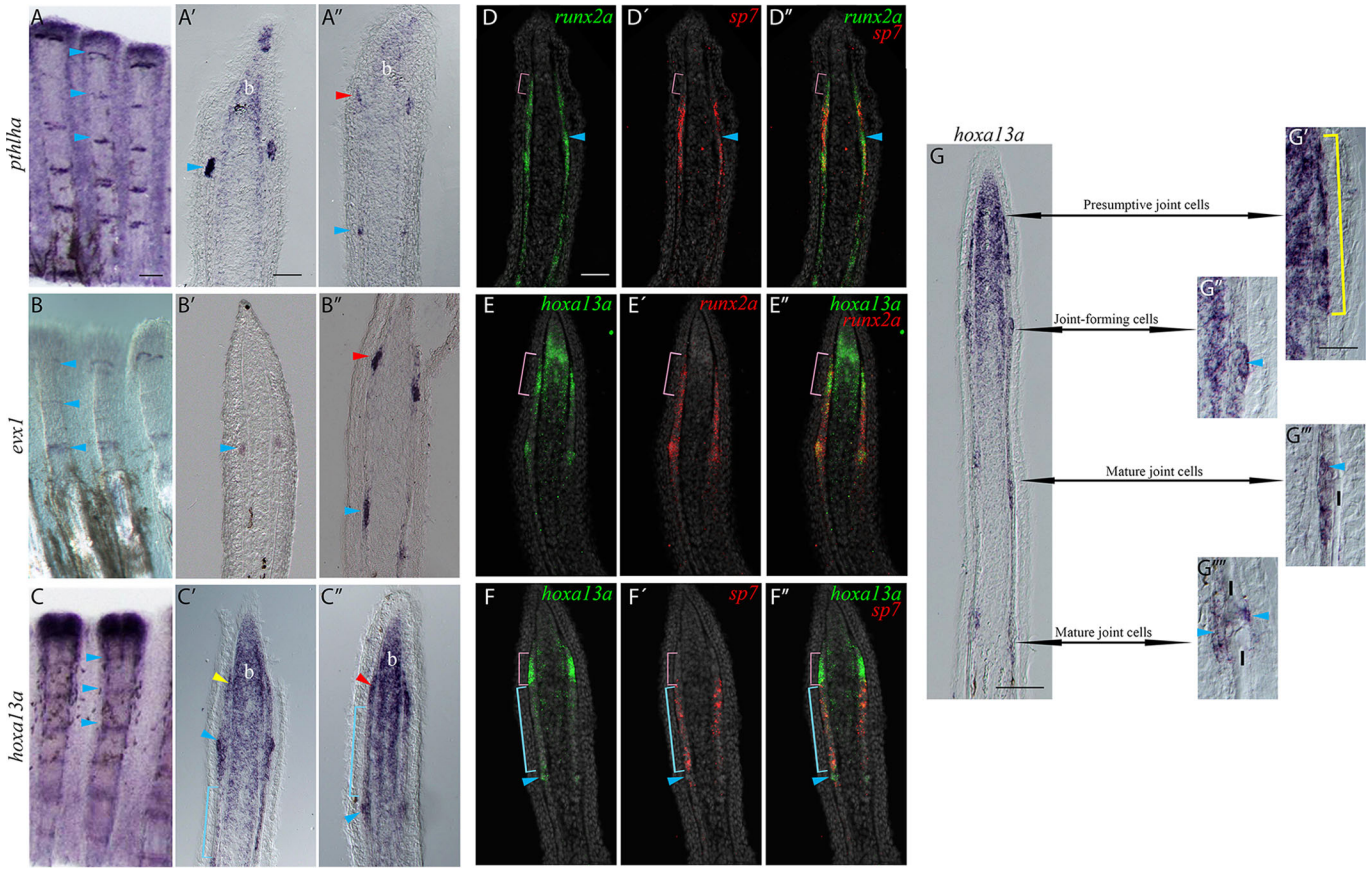

Fig. 3. Characterization of the presumptive joint cells. ISH or FISH on whole-mount (A-C) or longitudinal cryosections (A′-G⁗) at 4 dpa. A′-C′ and D-D″ show examples of rays without presumptive joint cells as indicated by a distance less than 200 µm between the joint-forming cells (blue arrowheads) and the distal edge of the pre-osteoblasts domain (pink brackets in D-D″). A″-C″ and E-G⁗ show examples of rays with presumptive joint cells: the distance between the joint-forming cells (blue arrowheads) and the distal pre-osteoblast domain (pink bracket) is about 254±25 µm. (A-C) *pthlha* (A), *evx1* (B) and *hoxa13a* (C) are expressed in joint regions. (A′-C′) The three markers are expressed in joint-forming cells and mature joints (blue arrowheads). Yellow arrowhead in C′ indicates pre-osteoblasts that lightly express *hoxa13a*. (A″-C″) An additional elongated domain of *pthlha* (A″), *evx1* (B″) and *hoxa13a* (C″) expression (red arrowheads) is observed distal to the joint-forming cells (blue arrowheads) in some rays. *hoxa13a* is also weakly expressed in newly committed osteoblasts (blue brackets in C′,C″). *hoxa13a* and *pthlha* are expressed in the blastema (A-A″,C-C″). (D-D″) A group of *runx2a*$^{+}$/*sp7*$^{-}$ pre-osteoblasts (pink brackets) is present distal to the *sp7*-expressing committed osteoblasts. (E-E″) Strong *hoxa13a* expression colocalizes with the distal edge of the *runx2a*-expressing pre-osteoblasts (pink brackets). (F-F″) Presumptive joint cells (pink brackets) and joint-forming cells (blue arrowheads) that strongly express *hoxa13a* lack *sp7* expression (pink brackets). However, *hoxa13a* is weakly expressed in newly committed *sp7*$^{+}$ osteoblasts (blue brackets). (G) ISH for *hoxa13a* expression illustrating changes in cell morphology as joints mature. (G′) The presumptive joint cell *hoxa13a* expression domain possesses an elongated shape (yellow bracket). (G″) The more proximal and mature “joint-forming cells” form a round cluster (blue arrowhead) that is distinct from osteoblasts. (G‴-G⁗) *hoxa13a* expression persists in mature joint cells, which are located first on the internal side (G‴), then on both internal and external sides (G⁗) of the lepidotrichia (blue arrowheads). b, blastema; l, lepidotrichia. Scale bars: 200 µm (in A for A-C); 50 µm (in A′ for A′-C″); 50 µm (in D for D-F); 100 µm (G); 30 µm (in G′ for G′-G⁗).

joint cells, characterized by a distance of less than 254±25 µm from the joint-forming cell cluster, *runx2a/sp7* double FISH revealed that the most distal *runx2a*-expressing domain lacks *sp7* expression (Fig. 3D-D″, Fig. S2J-J″). These *runx2a*$^{+}$/*sp7*$^{-}$ cells, which faintly express *hoxa13a* (Fig. 3C′), are pre-osteoblasts that have not yet committed to the osteoblast cell lineage. When presumptive joint cells were present, identified by a distance of 254±25 µm from the joint-forming cells (Fig. 3F), strong *hoxa13a* expression colocalized with the *runx2a*$^{+}$/*sp7*$^{-}$ pre-osteoblasts (Fig. 3E-F″). Therefore, *hoxa13a* expression increases in *runx2a*$^{+}$/*sp7*$^{-}$ pre-osteoblasts destined to become *pthlha/evx1/hoxa13a*-expressing joint cells. Overall, these results suggest that the distally located *runx2a*$^{+}$/*sp7*$^{-}$ cells can differentiate down the osteoblast lineage (through *sp7* expression) or commit to a joint cell type by expressing *pthlha*, *evx1* and *hoxa13a*.

This analysis reveals novel joint cell markers, *pthlha* and *hoxa13a*, and a previously unrecognized presumptive joint cell domain that correlates with the most distal pre-osteoblasts (Fig. 3G′). As the regenerate grows, presumptive joint cells form a cluster, becoming the ‘joint-forming cells’ (Fig. 3G″) (described in Fig. 1 and Fig. 3A′-C′). As the joint-forming cells mature, they become located on the internal side of the hemirays (Fig. 3G‴). More proximally, mature joint cells appear on both sides of the hemirays (Fig. 3G⁗). The three joint cell markers (*evx1*, *pthlha* and *hoxa13a*) are expressed throughout joint cell maturation.

Sequential expression of *hoxa13a*, *evx1* and *pthlha* in presumptive joint cells

Double FISH using combinations of *hoxa13a*, *evx1* and *pthlha* probes elucidated three distinct patterns of expression (Fig. 4). Patterns I and II were observed in rays with presumptive joint cells and Pattern III was observed in rays without presumptive joint cells. When presumptive joint cells were present, *hoxa13a* was strongly expressed either alone (Pattern I; Fig. 4A,C, Figs S3 and S5) or in

Development (2018) 145, dev161158. doi:10.1242/dev.161158

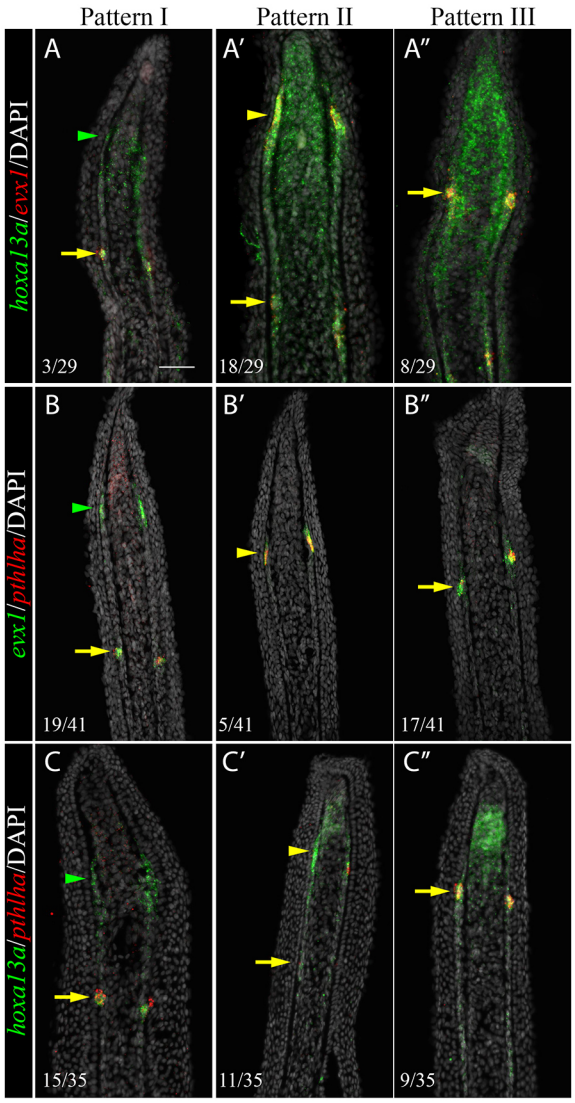

Fig. 4. Sequential activation of *hoxa13a*, *evx1* and *pthlha* expression in the presumptive joint cells. Double FISH and DAPI counterstains on longitudinal cryosections of 4 dpa fin regenerates illustrate three distinct patterns of expression. (A-C′) Patterns I and II are observed in rays with presumptive joint cells (arrowheads). (A″-C″) Pattern III is observed in rays without presumptive joint cells. (A-C″) In joint-forming cells (yellow arrows), the three markers are co-expressed in the joint-forming cells. (A,A′,C,C′) In the presumptive joint cells (green or yellow arrowheads), *hoxa13a* is expressed alone (Pattern I, A,C) or co-expressed with *evx1* (Pattern II, A′) or *pthlha* (Pattern II, C′). (B′,C′) *pthlha* is also co-expressed with *evx1* (B′). (B,B′) *evx1* is either expressed alone (B) or co-expressed with *pthlha* (B′). Numbers in each panel represent the number of sections with the expression pattern over the total number of sections analyzed. Scale bar: 50 µm (in A for A-C″).

combination with *evx1* (Pattern II; Fig. 4A′, Fig. S3) or *pthlha* (Pattern II; Fig. 4C′, Fig. S5). The *evx1* and *pthlha* genes were never expressed alone in double FISH that included *hoxa13a*. These data suggest that *hoxa13a* is the first marker to be strongly upregulated in presumptive joint cells. In *evx1/pthlha* double FISH, *evx1* was always expressed in the presumptive joint cells (Patterns I and II; Fig. 4B,B′, Fig. S4), and some sections exhibited *evx1* and *pthlha* co-expression (Pattern II; Fig. 4B′, Fig. S4). However, *pthlha* was never expressed alone. These data suggest that *evx1* expression is activated prior to *pthlha* in the presumptive joint cells. Overall, these data suggest that *hoxa13a* is upregulated first followed by the activation of *evx1* and then *pthlha* in presumptive joint cells. All three continued to be expressed in joint-forming cells (Pattern III; Fig. 4, Figs S3-S5).

To elucidate the genetic pathways associated with *hoxa13a*, *evx1* and *pthlha*, gene expression in 4 dpa fin regenerate sections was compared between wild type (Fig. 5A-C) and *evx1*$^{-/-}$ mutants (Fig. 5D-F) (Schulte et al., 2011). In *evx1*$^{-/-}$ mutants, *hoxa13a* expression persisted and *pthlha* expression was lost in the presumptive joint cells (Fig. 5E,F). Therefore, *evx1* lies downstream of or in parallel with *hoxa13a* and upstream of *pthlha* in presumptive joint cells. Furthermore, *hoxa13a* is potentially one of the initial factors expressed in presumptive joint cells. Interestingly, there was no joint-forming cell 'bump' in *evx1*$^{-/-}$ mutants and *hoxa13a* expression was absent proximal to the presumptive joint cells (data not shown). In *evx1*$^{-/-}$ mutants, the osteoblast markers *col10a1a* and *ihha* were expressed uniformly without the gaps corresponding to the joint-forming cells (Fig. S6A,B,D,E) but *ptch2* expression did not appear to be affected (Fig. S6C,F). These data suggest that the absence of Evx1 prevents *hoxa13a*-expressing presumptive joint cells from expressing *pthlha*. Joint-forming cells are not formed, resulting in the absence of joints in the fin regenerate.

Inhibition of calcineurin prevents joint formation and inhibits joint-related gene expression

Previous studies indicate that the mechanisms controlling fin growth and joint formation may be linked (Ton and Iovine, 2013). Furthermore, it has been suggested that calcineurin provides

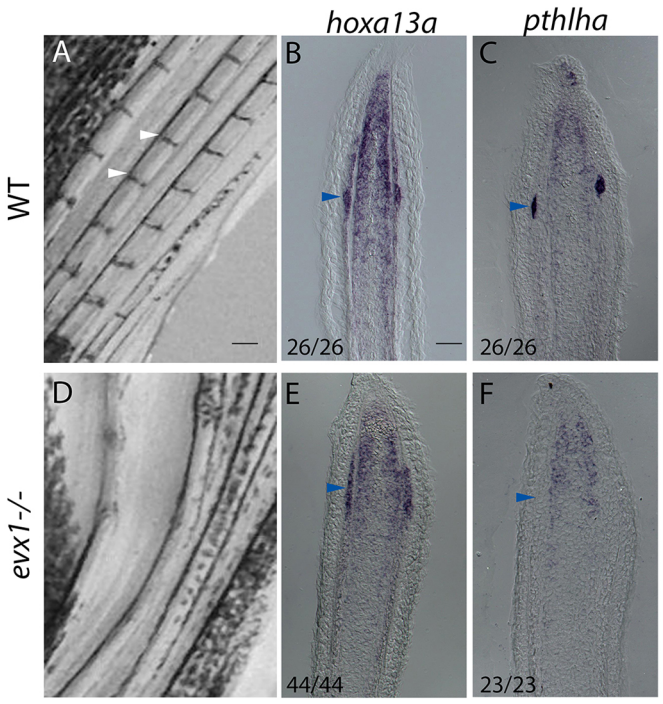

Fig. 5. In *evx1*$^{-/-}$ loss-of-function mutants, expression of *hoxa13a* but not *pthlha* persists in presumptive joint cells. (A) Wild-type fins possess joints (white arrowheads). (B,C) ISH on longitudinal cryosections of 4 dpa wild-type regenerates reveals *hoxa13a* (B) and *pthlha* (C) expression in joint cells (blue arrowheads). (D) In *evx1*$^{-/-}$ mutants joints are lost. (E,F) Longitudinal cryosections of 4 dpa *evx1*$^{-/-}$ mutant regenerates indicate *hoxa13a* (E) is expressed in presumptive joint cells but *pthlha* is not (F). Numbers in each panel represent the number of sections with the expression pattern over the total number of sections analyzed. Scale bars: 200 µm (in A for A,D); 50 µm (in B for B,C,E,F).

Development (2018) 145, dev161158. doi:10.1242/dev.161158

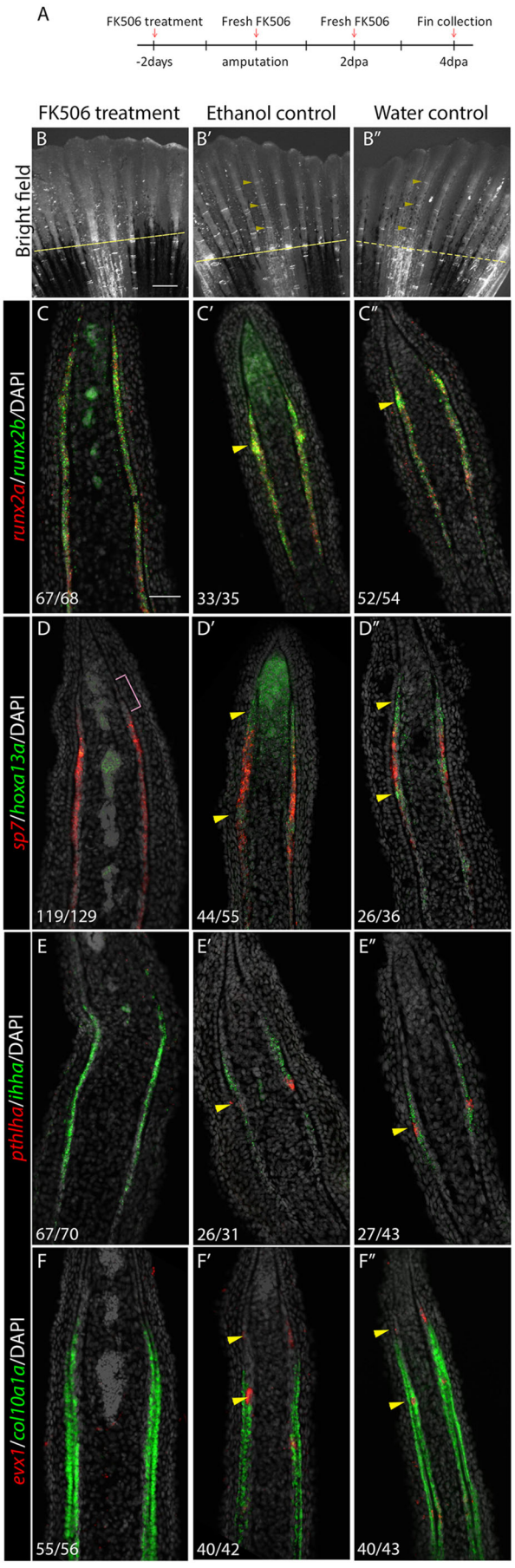

Fig. 6. Inhibition of calcineurin activity suppresses joint formation and joint-related gene expression. (A) Fish were treated with FK506 for 2 days prior to amputation. At 0 dpa/2 dot, fins were amputated and treatments continued for 4 days. (B) At 4 dpa/6 dot, no joints form in the regenerates of FK506-treated fish. (B′,B″) Ethanol (B′) and water (B″) controls form joints normally in the regenerate (yellow arrowheads). Dashed yellow lines indicate amputation plane. (C-F″) Double FISH on longitudinal cryosections of 4 dpa regenerates. (C) In FK506-treated fins, *runx2a* and *runx2b* are expressed, but joint cell clusters are absent (no 'bump' in the expression domain). (D-F) FK506 treatment inhibits *hoxa13a* (D), *pthlha* (E) and *evx1* (F) expression. *sp7* (D), *ihha* (E) and *col10a1* (F) domains of expression are uninterrupted in committed osteoblasts owing to the absence of joints. However, *sp7* is still absent in the distal pre-osteoblasts (D, pink bracket). (C′-F″) Expression of joint (yellow arrowheads) and osteoblast markers are unaffected in ethanol (C′-F′) and water (C″-F″) controls. Numbers in each panel represent the number of sections with the expression pattern over the total number of sections analyzed. Scale bars: 500 µm (in B for B-B″); 50 µm (in C for C-F″).

positional information through the inhibition of RA signaling to regulate regenerate outgrowth (Kujawski et al., 2014). To determine the effects of a disruption of positional information on joint formation, fish were treated with 0.1 µg/ml FK506 (also known as tacrolimus or fujimycin). Following 2 days of treatment (dot), fins were amputated and treatment was continued for 4 days (Fig. 6A). At 4 dpa/6 dot, no joints were visible in regenerates of FK506-treated fish (n=12) (Fig. 6B). Joints formed normally in 4 dpa regenerates of untreated (n=12) and ethanol control fish (n=12) (Fig. 6B′,B″). These data indicate that calcineurin affects joint formation during regeneration.

Double FISH on 4 dpa/6 dot regenerates indicate that FK506 treatment inhibits *evx1*, *pthlha* and *hoxa13a* expression (Fig. 6D-F″). Furthermore, features associated with joint-forming cells such as the 'bump' of *runx2a/b* expression and the *sp7*/*col10a1a*/*ihha* gap in expression were consistently absent in FK506-treated fish (Fig. 6C-F). However, the distal group of *runx2a/b*$^{+}$/*sp7*$^{-}$ pre-osteoblasts persisted in FK506-treated fish (Fig. 6D). Overall, these data indicate that *runx2*$^{+}$/*sp7*$^{-}$ distal pre-osteoblasts are present following FK506 treatment, but are only able to differentiate into osteoblasts.

Retinoic acid inhibits the expression of joint cell markers and induces ectopic bone deposition in mature joints

A previous study proposed that calcineurin inhibition promotes RA signaling (Kujawski et al., 2014). Gene expression analysis indicates that *retinoic acid receptor, gamma b* (*rargb*) is expressed in joint-forming and mature joint cells, suggesting that these cells can respond to RA signaling (Fig. S7A-B). Therefore, we investigated how RA treatment affects joint cell marker expression. RA treatment (1 µM) for 1 day starting at 3 dpa led to the loss of *evx1*, *pthlha* and *evx1* in all joint cells of the regenerates (Fig. 7A, B-D) compared with ethanol and water controls (Fig. 7B′-D′,B″-D″). Because RA treatment impairs fin regeneration (data not shown), its effect on new segment formation could not be assessed. Therefore, the effect of RA on mature joints was analyzed.

An *in vivo* double-staining procedure for calcified tissue was used to assess new bone matrix deposition during RA treatment. Fish were stained *in vivo* with Alizarin Red at 7 dpa and then RA treatment (1 µM) was initiated. Fish were stained with calcein at 6 dot/13 dpa and one mature joint (the first joint proximal to the first bifurcation on the second-most dorsal ray) was evaluated (Fig. 8A). New bone matrix, identified by calcein staining only, was observed in joint regions of RA-treated fish (Fig. 8B-D). No calcein staining was observed in joint regions of ethanol or

Development (2018) 145, dev161158. doi:10.1242/dev.161158

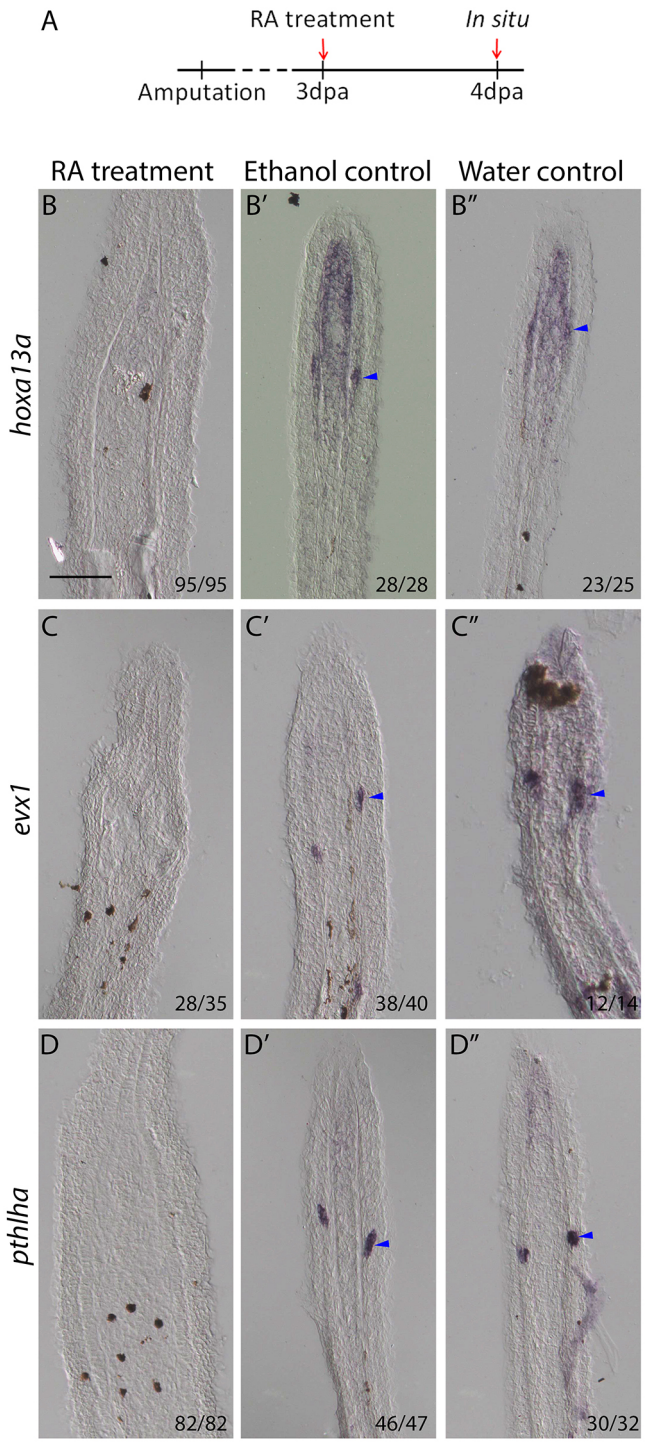

Fig. 7. RA treatment leads to the inhibition of joint cell marker expression. (A) Fish were treated with RA from 3 to 4 dpa. (B-D) ISH on longitudinal cryosections at 4 dpa/1 dot indicate *hoxa13a* (B), *evx1* (C) and *pthlha* (D) expression are lost in joint cells of RA-treated fish. (B′-D″) Expression remains in joint cells (blue arrowheads) of ethanol (B′-D′) and water (B″-D″) controls. Numbers in each panel represent the number of sections with the expression pattern over the total number of sections analyzed. Scale bar: 100 µm (in B for B-D″).

water controls (Fig. 8B′-D′,B″-D″). These data indicate that bone matrix was deposited in joints following RA treatment. Similar results were observed in intact fins following RA treatment (6 dot) (Fig. S7C-C″).

To determine whether mature osteoblasts were present in joint regions, *Tg(bglap:mCherry)* fish were treated with RA for 6 days starting at 7 dpa (Fig. 8E). Prior to RA treatment, well-defined gaps in mCherry-expressing osteoblasts were observed in joint regions (Fig. 8F, Fig. S7D-D″). However, at 6 dot/13 dpa, mCherry-expressing osteoblasts were present in joint spaces of RA-treated fish, narrowing or filling the gaps (Fig. 8G, Fig. S7E). No changes were observed in control groups (Fig. 8F′,F″,G′,G″, Fig. S7E′-E″). These observations suggest that RA treatment results in either the differentiation of joint cells into osteoblasts, or joint cell death allowing surrounding osteoblasts to fill joint spaces and deposit bone matrix. However, terminal deoxynucleotidyl transferase dUTP nick end labeling assays following 24 h of RA treatment did not detect any significant cell death in joint cells or osteoblasts (data not shown).

RA treatments can induce joint cells to differentiate into osteoblasts

To determine whether RA induces the differentiation of joint cells into osteoblasts, RA treatments were performed on intact fins of double transgenic zebrafish, *Tg(m-Inta11:eGFP; bglap:mCherry)*. The reporter line *Tg(m-Inta11:eGFP)* recapitulates *hoxa13a* expression in adult fin rays as shown by EGFP expression in joint cells of intact and regenerating rays (Fig. 9A-C). Although RA suppressed *hoxa13a* expression, some EGFP persisted owing to its half-life of 24 h (Thomas et al., 2012). Following 3 days of RA treatment, EGFP-positive joint cells of *Tg(m-Inta11:eGFP; bglap:mCherry)* fish co-expressed mCherry in joint regions (35/44 joints observed in six fish) (Fig. 9D-G, Fig. S7F-F3). No mCherry-expressing cells were observed in controls (Fig. 9D′-G′,D″-G″). These data indicate that joint cells differentiate into osteoblasts following RA treatment.

DISCUSSION

During fin regeneration, cells that come into contact with the epidermis differentiate into osteoblasts or joint cells, enabling the formation of bone segments at the end of each ray. Using gene expression and functional analyses, a regulatory mechanism of joint cell specification during fin regeneration has been elucidated (Fig. 10). We propose the following model for joint formation. In the distal fin regenerate, *runx2a/b*$^{+}$*/sp7*$^{-}$ cells are committed to either a joint or osteoblast cell fate. Upon *sp7* expression, cells are committed to an osteoblast fate (Nakashima et al., 2002). However, *runx2a/b*$^{+}$*/sp7*$^{-}$ cells that strongly express *hoxa13a*, do not differentiate into osteoblasts and instead become joint cells. These previously unrecognized presumptive joint cells mature as regeneration continues and begin to express *evx1*. Evx1 acts downstream of or in parallel with *hoxa13a*, but upstream of *pthlha*. As regeneration continues, joint-forming cells continue to express the three markers. Treatment with the calcineurin inhibitor FK506 inhibited joint formation and the expression of *evx1*, *pthlha* and *hoxa13a*. Already, it has been shown that FK506 activates RA signaling (Kujawski et al., 2014). We showed that RA treatment inhibits *evx1*, *pthlha* and *hoxa13a* expression. As *hoxa13a* is an early marker for presumptive joint cells, calcineurin activity may act to inhibit RA signaling, which regulates *hoxa13a* expression in presumptive joint cells. Furthermore, RA treatment induced the differentiation of joint cells into osteoblasts, which deposit bone matrix in mature joints. These data suggest that RA levels must be tightly controlled for joint formation and maintenance in the fin regenerate.

Development (2018) 145, dev161158. doi:10.1242/dev.161158

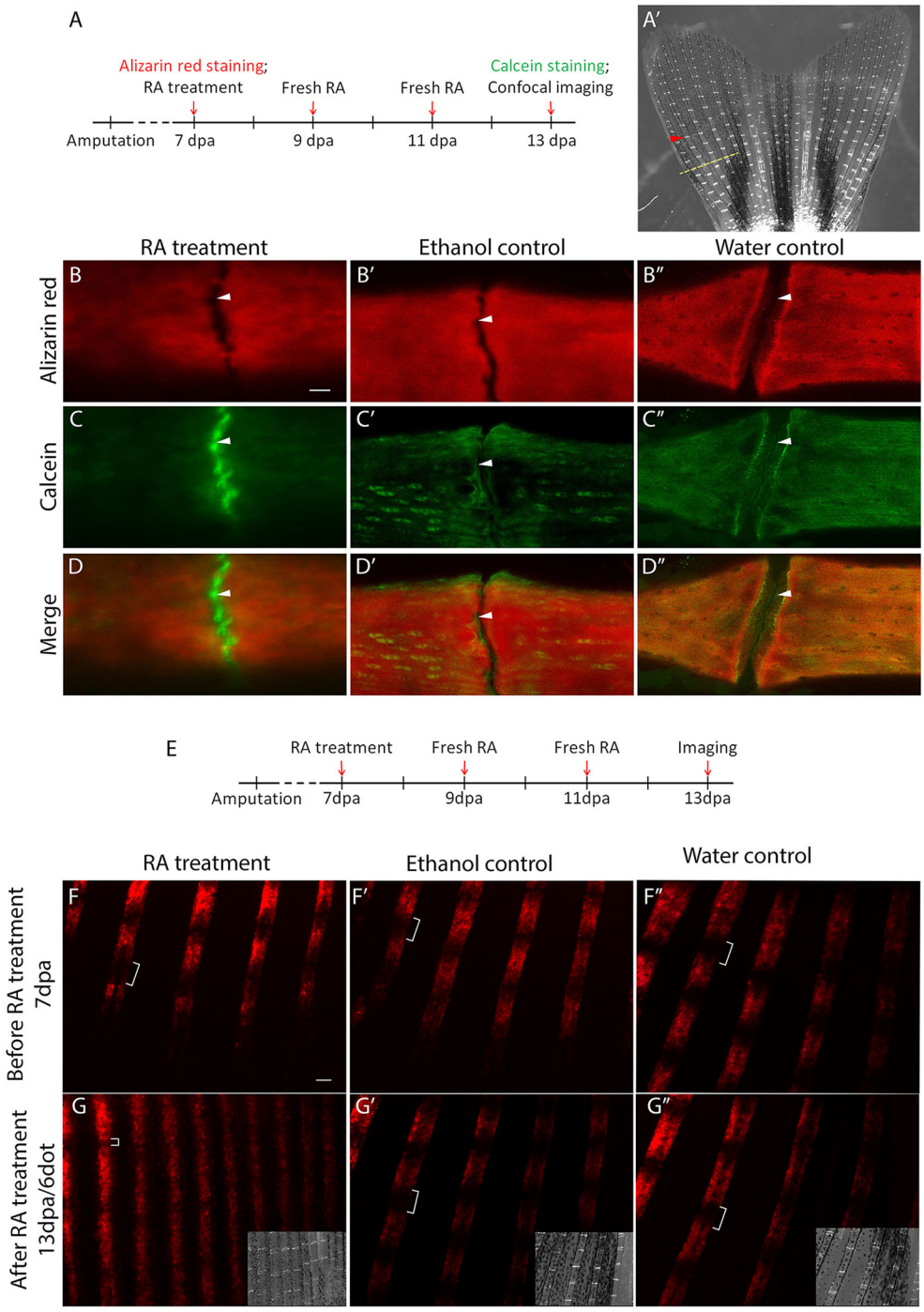

Fig. 8. RA treatment leads to bone matrix deposition between bone segments. (A) Fish with regenerating fins (7 dpa) were stained with Alizarin Red, and then treated with RA for 6 days. At 6 dot/13 dpa, fins were stained with calcein. (A′) The first joint proximal to the first bifurcation on the second most dorsal fin ray was analyzed (red arrowhead). Yellow dashed line indicates amputation plane. (B-B″) Alizarin Red staining alone shows no difference between RA-treated and control joints (white arrowheads). (C) Calcein staining indicates new bone matrix being deposited within joint spaces (white arrowhead) following RA treatment. (C′,C″) No new bone is observed in ethanol (C′) and water (C″) controls (white arrowheads). (D′-D″) Merged images of Alizarin Red and calcein staining. (E) *Tg*(*bglap:mCherry)* fish at 7 dpa were treated with RA for 6 days and imaged. (F-F″) At 0 dot/7 dpa (before RA treatment), mature osteoblasts are not observed in joint regions of fin regenerates (white brackets). (G) At 6 dot/13 dpa, a decrease in gap size (white brackets) is observed in RA-treated fish compared with ethanol (G′) and water (G″) controls. Insets in G-G″ are bright-field images to show the ray joints. Scale bars: 10 µm (in B for B-D″); 100 µm (in F for F-G″).

Joint cells and osteoblasts originate from a distal *runx2*-positive subset of cells

Gene expression analysis has shown that a group of *runx2a*$^{+}$/*sp7*$^{-}$ cells is present distal to the *sp7*-expressing committed osteoblasts (Fig. 3D-D″). As these cells do not strongly express any joint cell markers or the osteoblast commitment marker, it is possible that these cells are bipotent and can differentiate into either osteoblasts or become presumptive joint cells. In mice, it has been shown that *Runx2*-expressing pre-osteoblasts are bipotent cells that can differentiate into either osteoblasts or chondrocytes. However, upon expression of *Sp7*, cells are committed to an osteoblast fate (Nakashima et al., 2002). Conversely, a loss of *Sp7* in the long bones of mice causes ectopic cartilage formation, potentially due to a fate switch of osteoblast progenitors to chondrocytes (Nakashima et al., 2002). Therefore, *runx2*-positive cells lacking joint markers and *sp7* are also potentially bipotent cells. These results are supported by previous studies using clonal analysis and lineage tracing that suggest osteoblasts may contribute to joint cells (Ando et al., 2017; Tu and Johnson, 2011). Another study showed that upon ablation of osteoblasts, the rays regenerate normally, suggesting a potential transdifferentiation mechanism through an unknown source to replace the osteoblasts (Singh et al., 2012). Assuming a common cell origin and that joint cells are a separate differentiated cell type from osteoblasts, these cells could potentially commit to the alternative cell type and transdifferentiate during regeneration. Therefore, joint cells may be the elusive

Development (2018) 145, dev161158. doi:10.1242/dev.161158

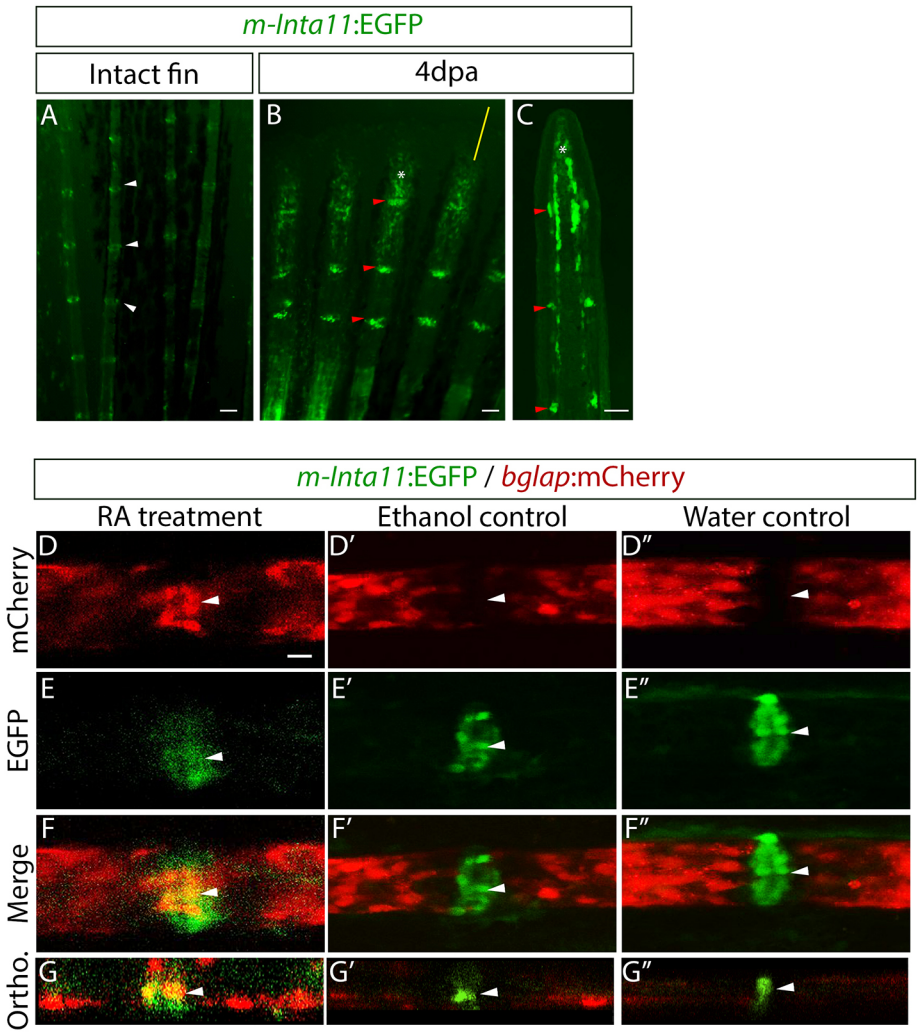

Fig. 9. RA treatment leads to the differentiation of joint cells to mature osteoblasts. (A-C) *Tg(m-Inta11-EGFP)* GFP reporter expression in the intact fin (A) and 4 dpa regenerate (B,C). (A) Whole-mount intact fins illustrate that EGFP is expressed faintly in osteoblasts and strongly in joint cells (white arrowheads). (B,C) Whole-mount (B) and longitudinal sections (C) of regenerating fins show EGFP expression in joint cells (red arrowheads) and in osteoblasts and the blastema (white asterisks). Yellow line in B indicates the position of the section shown in C. (D-G) Confocal images of RA-treated *Tg(m-Inta11:EGFP; bglap:mCherry)* fin regenerates at 3 dot illustrates that EGFP-expressing joint cells begin to express mCherry (white arrowheads). (D′-F″) Ethanol (D′-F′) and water (D″-F″) controls indicate that EGFP-positive joint cells do not express mCherry (white arrowheads). (G-G″) Orthogonal view through the fin ray showing co-expression of EGFP and mCherry in joint cells (white arrowheads). Scale bars: 50 µm (A-C); 10 µm (in D for D-F″).

potential alternative source of osteoblasts that was hypothesized in the cell ablation study (Singh et al., 2012).

Given that these cells are of a common cell origin, it is possible that joint cells differentiate into a separate cell type or are the result of an arrest in osteoblast differentiation. Joint cells can be considered a differentiated cell type as they express genes that are not expressed in osteoblasts. Indeed, they do not keep the transcript signature that they had at the time when *evx1* and *pthlha* are expressed. For example, they do not express *sp7*, and they downregulate *runx2a/runx2b* (Knopf et al., 2011). Alternatively, it is possible that joint cells are the result of an arrest in osteoblast differentiation. Previously, it has been shown that maintenance of synovial joint articular cartilage in humans and mice depends on the inhibition of chondrocyte differentiation (Drissi et al., 2005; Lotz et al., 1999; Serra et al., 1997, 1999). Furthermore, chondrocyte maturation is arrested and cartilage matrix genes are repressed in the developing zebrafish hyoid joint (Askary et al., 2015). The inability to maintain chondrocytes in an immature state results in hyoid joint

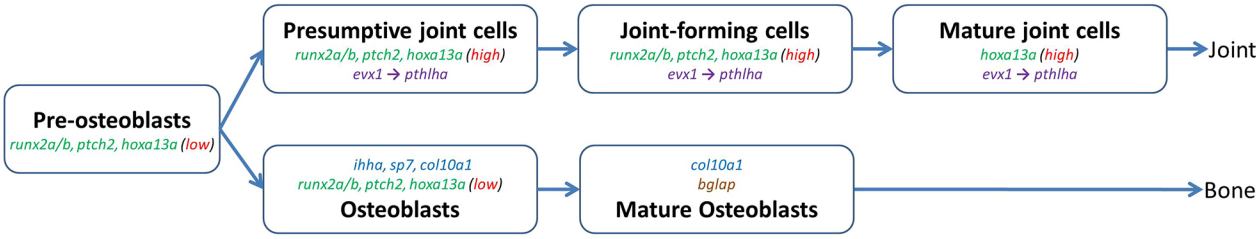

Fig. 10. Model of joint cell differentiation pathway. Pre-osteoblasts express *runx2a*, *runx2b*, and low levels of *hoxa13a*. The upregulation of *hoxa13a* correlates with the formation of presumptive joint cells and subsequent expression of *evx1*, which is upstream of *pthlha*. *hoxa13a*, *evx1* and *pthlha* continue to be expressed in joint-forming and mature joint cells and a joint is formed. In the absence of *hoxa13a* upregulation, *sp7* is expressed and cells are committed to the osteoblast cell lineage. Committed osteoblasts then express osteoblast markers such as *ihha* and *col10a1a*. Committed osteoblasts then mature and begin to express *bglap*. *ihha* is not expressed in joint cells, but pre-osteoblasts, joint-forming cells, and osteoblasts all express *ptch2*. Similar to endochondral ossification, it is possible that there is a feedback loop between *pthlha* and *ihha*. Different colors illustrate factors expressed in all three cell types (green) and the ones only expressed in osteoblasts (blue), joint cells (purple) and mature osteoblasts (brown).

Development (2018) 145, dev161158. doi:10.1242/dev.161158

fusions (Askary et al., 2015). Therefore, the joint markers *hoxa13a*, *evx1* and *pthlha* may act to repress osteoblast differentiation. As these cells do not express *col10a1a* or *bglap*, they are unable to deposit bone matrix and joint cavities are formed. Consequently, the absence of the joint markers (i.e. Evx1) may result in continued differentiation down the osteoblast pathway leading to a single bone segment.

Joint cells express *pthlha*, a potential inhibitor of osteoblast differentiation

Joint-forming cells express *pthlha*, but do not express *ihha*. However, *pthlha*-expressing joint cells express *ptch2*, indicating that Hedgehog signaling is active in these cells. Furthermore, we show that *pth1ra* is expressed in joint cells and osteoblasts, indicating that Pthlha signaling is active in these cells. Currently, the roles of these factors in the fin regenerate are unknown. However, *pthlha* can inhibit osteoblast differentiation during intramembranous ossification in mouse and endochondral ossification in zebrafish (Abzhanov et al., 2007; Lenton et al., 2011; Yan et al., 2012). Therefore, *pthlha* may inhibit osteoblast differentiation in fin ray joint cells. Analysis of *ihha* and *ptch2* zebrafish mutants indicate that Hh signaling is required for the recruitment and proliferation, but not differentiation, of *runx2a/2b*-expressing pre-osteoblasts to the growing edge of the opercle dermal bone (Huycke et al., 2012). However, *ihha* mutants display fusions between opercular intramembranous bones that form functional articulations, suggesting that Ihha may play a role in maintaining joint identity (Hulsey et al., 2005; Huycke et al., 2012). Currently, whether *ihha* and *pthlha* interact during intramembranous ossification is unknown. However, it has been established in mouse and chick studies that a negative-feedback loop occurs between PTHrP and Ihh during endochondral ossification to allow precise control over chondrocyte proliferation and differentiation (Kobayashi et al., 2002; Kronenberg, 2003; Lanske et al., 1996; Long et al., 2004; St-Jacques et al., 1999; Vortkamp et al., 1996; Zhao et al., 2002). Considering the previously established roles for Ihh and PTHrP during endochondral and intramembranous ossification in mouse and chick, it is possible that *pthlha* negatively regulates *ihha* expression in joint-forming cells and presumptive joint cells to promote a joint cell identity and/or inhibit osteoblast differentiation. As Hedgehog signaling is active in joint-forming cells, it is possible that Ihha signals joint-forming cells to promote *pthlha* expression. However, because Shha is expressed in cells adjacent to *ptch2*-expressing joint cells (Laforest et al., 1998; Quint et al., 2002; Smith et al., 2006), one cannot discount the possibility that Shha also contributes to joint formation in an as-yet-unknown mechanism.

hoxa13a is involved in joint formation

We show that *hoxa13a* is strongly expressed in joint cells at all maturation stages. In addition, *hoxa13a* is also weakly expressed in pre-osteoblasts and a small number of newly committed osteoblasts. Previous mathematical models proposed that joint formation triggers the production of a joint-inhibiting factor in close proximity (Rolland-Lagan et al., 2012). As regeneration continues, the distance from the last-formed joint increases and the concentration of the inhibiting factor decreases, allowing the reactivation of joint-inducing factors that may include *hoxa13a*. We propose that when the concentration of Hoxa13a reaches a certain threshold, distal *runx2a/b*-positive cells are committed to become joint cells and express *evx1*.

In embryonic day 14.5 mouse limbs, *Hoxa13* is expressed in the peridigital tissues and interarticular digit condensations (Stadler et al., 2001). Furthermore, *Hoxa13* loss-of-function mutants show a number of autopod defects, most notably the absence and fusion of phalangeal segments (Fromental-Ramain et al., 1996; Knosp et al., 2004; Perez et al., 2010). These autopod defects are suggested to be caused in part by the misregulation of genes involved in cell sorting, boundary formation, and cell adhesion (Stadler et al., 2001). More specifically, mesenchymal cells lacking *Hoxa13* are unable to attach efficiently to cell culture dishes and self-aggregate *in vitro* (Stadler et al., 2001). However, in the presence of wild-type cells, *Hoxa13*$^{-/-}$ cells are able to form aggregates and undergo chondrocyte differentiation (Stadler et al., 2001). Furthermore, *Hoxa13* has been shown to mediate perichondrial boundary formation in mouse limbs, restricting the mixing of heterogeneous mesenchymal cell populations (Stadler et al., 2001). Given that joint-forming cells in the fin regenerate segregate from the pre-osteoblast cells and form a cell cluster adjacent to differentiating osteoblasts, it is possible that *hoxa13a* regulates genes involved in cell sorting and adhesion in the fin regenerate and/or may regulate genes to prevent the intermingling of joint cells with the surrounding mesenchymal cell population.

Calcineurin, through RA signaling, regulates *hoxa13a* expression in presumptive joint cells

Fish treated with FK506 do not express *hoxa13a*, *evx1* or *pthlha* and fail to form joints. Previous mathematical modeling suggested that unknown opposing morphogen gradients and a joint-suppressing factor (potentially Cx43) regulate joint formation along the proximal-distal axis (Rolland-Lagan et al., 2012). It is known that FK506 treatment increases *cx43* expression, which negatively influences *evx1* expression and inhibits joint formation (Dardis et al., 2017). FK506 also expands distal gene expression domains to make them appear similar to more proximal gene expression domains (Kujawski et al., 2014). Therefore, FK506 treatment may disrupt the aforementioned opposing morphogen gradients, further inhibiting joint formation. Furthermore, FK506 studies have shown that calcineurin signaling may act to inhibit RA signaling pathway during fin regeneration (Kujawski et al., 2014). Our studies indicate that RA treatment also inhibits *pthlha*, *hoxa13a* and *evx1* expression in all joint cells of the fin regenerate. In mature joint cells, the RA-induced loss of *pthlha*, *hoxa13a* and *evx1* is accompanied by the differentiation of joint cells into osteoblasts and ectopic bone deposition. The ability of joint cells to differentiate into mature osteoblasts suggests that either an arrest in osteoblast differentiation was lifted or joint cells were able to transdifferentiate into osteoblasts.

MATERIALS AND METHODS

Animals

All fish used in the experiments were maintained at 28°C with a photoperiod of 14 h of light and 10 h of darkness. Fish were fed regularly (Westerfield, 2007). Homozygous *evx1*^{i232} mutant fish were a gift from Dr Katherine E. Lewis (Schulte et al., 2011). The *bglap* regulatory fragment was acquired from Dr Christoph Winkler and subcloned in a Tol2 vector to make the *bglap:mCherry* construct, which was then used to create a new transgenic line. The *Tg(m-Inta11:eGFP)* line was previously described (Kherdjemil et al., 2016). All experiments were performed according to the Canadian Council on Animal Care guidelines.

Fin amputations

Zebrafish were anesthetized by immersion in system water containing 0.17 mg/ml tricaine (Westerfield, 2007). Caudal fins were amputated two segments proximal from the first branch point of the lepidotrichia; this is

Development (2018) 145, dev161158. doi:10.1242/dev.161158

referred to as a standard cut. Fish were then returned to a fresh system water to recover.

Live imaging

Fish were anesthetized and placed on a 1% agarose plate with the caudal fins spread out naturally (adults). The plate was placed under a Leica MZ FLIII dissection microscope and images were taken using an AxioCam HSM digital camera and AxioVision AC software (Carl Zeiss). For live confocal imaging, fish were anesthetized and immersed in 0.17 mg/ml tricaine in a Petri dish. The caudal fins were flattened to the bottom of the Petri dish with a slice hold-down (Warner Instruments, 64-0248) and imaged with a water-immersion objective on a Nikon A1RsiMP confocal microscope. All images were processed using ImageJ (NIH).

In situ hybridization

In situ hybridizations (ISH) on longitudinal cryosections of at least three adult fin regenerates per probe were performed as previously described (Smith et al., 2008) with modifications. Briefly, fin samples were fixed with 4% paraformaldehyde (PFA) overnight at 4°C and cryosectioned at 20 µm. Sections were stored at −20°C until use. On day one of ISH, slides were thawed at 60°C for 1 h. Sections were permeabilized with 0.3% Triton X-100 in PBS for 15 min and then with 5 µg/ml proteinase K for 15 min at room temperature. Sections were post-fixed with 4% PFA in PBS to prevent them from detaching from the slides, and acetylated with 1.25% triethanolamine and 0.3% acetic anhydride. Each slide was then covered with 500 µl hybridization buffer [1× salt solution (0.2 M NaCl, 10 mM Tris-HCl, 5 mM NaH_2PO_4, 5 mM Na_2HPO_4, 1 mM Tris-base, 5 mM EDTA), 50% deionized formamide, 10% dextran sulfate, 1 mg/ml yeast tRNA and 1× Denhardt's solution] containing approximately 1 ng/µl RNA probe and hybridized overnight at 70°C. On day two, slides were washed 2×30 min with 1× SSC, 50% formamide and 0.1% Tween-20 and then 2×30 min with TBST [140 mM NaCl, 2.7 mM KCl, 25 mM Tris HCl (pH 7.5), 0.1% Tween 20]. Slides were then blocked with 10% calf serum in TBST and incubated with anti-digoxigenin (DIG) at 1:2000 overnight at 4°C. On day three, slides were first washed 6×20 min with TBST and then stained in a Coplin jar containing 40 ml NTMT (100 mM NaCl, 100 mM Tris-HCl pH 9.5, 50 mM $MgCl_2$ and 0.1% Tween-20) with 225 µg/ml NBT and 175 µg/ml BCIP. The staining was performed at 37°C to accelerate the reaction. After staining, the slides were washed with water and mounted for observation.

Antisense RNA probes for *evx1* (Thaëron et al., 2000), *ihha* (Avaron et al., 2006), *hoxa13a* (Ahn and Ho, 2008), *col10a1a* (Padhi et al., 2004), *ptch2* (Concordet et al., 1996), *runx2a* and *runx2b* (Smith et al., 2006), and *sp7* (Li et al., 2009) were synthesized as previously described. *pthlha* (693 bp) was amplified using *pthlha* forward 5′-ggggacatcatcatcatcatcatc-3′ and *pthlha* reverse 5′-agcatttaggcgtcacaagtcctc-3′ primers and inserted into pDrive, linearized with *Xho*I, and transcribed *in vitro* with T7 RNA polymerase. *pth1ra* (654 bp) was amplified using *pth1ra* forward 5′-ggcctggaacagaaggactc-3′ and *pth1ra* reverse 5′-attcacgtccccacaatgct-3′ primers and cloned into pDrive. *pth1ra* was then linearized with *Bam*HI and transcribed *in vitro* with Sp6 RNA polymerase. *rargb* was amplified with primers 5′-tacaaaccctgcttcgtgtgcca-3′ and 5′-ccggattctccagcatctctctg-3′, and cloned into pDrive. The construct was then linearized with *Hin*dIII and transcribed with T7 polymerase.

Double fluorescence *in situ* hybridization (FISH) on sections

Double FISH on longitudinal cryosections of adult fin regenerates was adapted from protocols that were previously described [Welten et al., 2006; manufacturer's protocols for TSA Cyanine 3 (PerkinElmer, NEL753001KT) and Fluorescein TSA Cyanine 5 systems (PerkinElmer, NEL745001KT)]. Fin regenerates were fixed and sectioned as described above. Permeabilization, hybridization and post-hybridization washes on sections were also performed as described above. After washing with TBST on day two, slides were washed with 2% H_2O_2 in TNT (0.1 M Tris-HCl pH 7.5, 0.15 M NaCl, 0.5% Tween20) for 10 min and then washed 4×5 min in TNT, blocked for 4 h in TBSTB (TNT with 0.5% PerkinElmer blocking powder), and incubated overnight in anti-DIG-POD (1:500) (Roche) in TBSTB at 4°C. Slides were then washed in TNT (6×20 min), stained with Tyr-Cy3 (1:100) in amplification diluent (PerkinElmer) for 10 min, and washed in TNT (3×5 min). Slides were then washed with 2% H_2O_2 in TNT for 30 min to eliminate the peroxidase of anti-DIG and washed and blocked as the previous day. Slides were then incubated overnight with anti-DNP-POD (1:500) (PerkinElmer) at 4°C. Slides were then washed in TNT (6×20 min), stained with Tyr-Fluorescein (1:100) in amplification diluent (PerkinElmer) for 10 min, and washed in TNT (3×5 min). Slides were then incubated in DAPI stock solution (5 mg/ml) diluted to 1:10,000 with TNT (1×5 min), washed in TNT (3×5 min), washed briefly with water, and mounted with AquaPolymount.

FK506 (tacrolimus) treatments

FK506 (tacrolimus) (Sigma-Aldrich, F4679) was dissolved in ethanol and added to system water at 0.1 µg/ml; this concentration was chosen based on published data (Kujawski et al., 2014). Fish were treated with FK506 for 2 days prior to fin amputation to ensure the chemical had time to take effect. Following 2 days of treatment (dot), fins were amputated and allowed to regenerate for 4 days. Every 2 days, the water was changed with fresh drug. Zebrafish were fed and kept in glass tanks throughout treatments. Control tanks contained either the same percentage of ethanol or system water alone. Each experiment was performed in triplicate (four fish per tank per experiment).

Retinoic acid treatments

RA treatment was adapted from Jeradi and Hammerschmidt (2016). A range of concentrations (0.5-10 µM) of RA were tested and 1 µM was the concentration that induced phenotype without causing mortality. A stock of RA (Sigma-Aldrich, R2625) was prepared by dissolving RA powder in DMSO to obtain a final concentration of 10 mM. This stock solution was diluted to 1 mM with ethanol and further diluted to 1 µM with system water. Zebrafish were kept in this solution in 2-l plastic tanks (four fish per tank per experiment) at 28.5°C in the dark with an air bubbler throughout treatments. RA solution was changed every 2 days during the period of the experiments. Control groups were left to swim in the 0.001% ethanol and 0.0001% DMSO or system water alone.

In vivo Alizarin Red and calcein staining

The Alizarin Red staining solution was prepared by dissolving Alizarin Red (Sigma-Aldrich, A-5533) directly into fish water to obtain a final concentration of 100 mg/l. The solution was also supplemented with 1 mM HEPES (Carl Roth). Calcein solution was prepared by dissolving calcein powder (Sigma-Aldrich) in fish water to obtain a final concentration of 100 mg/l. The pH for each staining solution was adjusted to 6.5. Fish were left to swim in the dark in Alizarin Red solution or calcein staining solution at 28.5°C for 1 h. Subsequent to staining, fish were washed three times for 5 min each wash in fish water. Alizarin Red staining was performed on wild-type fish prior to RA treatment and imaging. Calcein staining was performed following treatments and prior to imaging.

Immunohistochemistry

Fin regenerates were fixed in 4% paraformaldehyde overnight at 4°C and cryosectioned as previously described (Smith et al., 2006). Zns5 immunohistochemistry was adapted from a protocol that was previously described (Smith et al., 2006). Longitudinal cryosections of 4 dpa fin regenerates were incubated with Zns5 (ZFIN) monoclonal antibody (1:200). Fluorescently labeled secondary antibodies Alexa Fluor 488 goat anti-mouse IgG (H+L) (Invitrogen, A11001) were used at 1:500. Slides were counterstained with DAPI and mounted.

RT-PCR

Total RNA was extracted from 10 adult caudal fins or 50 embryos (1 dpf) using Trizol according to the manufacturer's protocol. Total RNA was checked for purity (Nanodrop) and integrity (agarose gel). Total RNA (1 µg) was reverse transcribed with the QuantiTect Reverse Transcription Kit (Qiagen) according to the manufacturer's instructions. PCR was performed using the primers listed in Table S1.

Acknowledgements

The work reported here benefited from the valuable assistance of Derek Sheppard, Ali Al-Rewashdi and Vishal Saxena. We thank Dr Katharine Lewis for providing

the *evx1* mutant and Dr Brian F. Eames for discussion of topics discussed in this paper. We would also like to thank Dr Marc Ekker for critical reading of the manuscript.

Competing interests
The authors declare no competing or financial interests.

Author contributions
Conceptualization: S.C.M., J.Z., S.J., M.H., M.-A.A.; Methodology: S.C.M., J.Z., S.J.; Investigation: S.C.M., J.Z., H.-E.P., L.P.; Writing - original draft: S.C.M.; Writing - review & editing: J.Z., M.H., M.-A.A.; Visualization: J.Z.; Supervision: M.H., M.-A.A.; Project administration: J.Z., M.-A.A.; Funding acquisition: M.-A.A.

Funding
This study is supported by funding from Canadian Institutes of Health Research (312217 to M.-A.A.).

Supplementary information
Supplementary information available online at
http://dev.biologists.org/lookup/doi/10.1242/dev.161158.supplemental

References
Abzhanov, A., Rodda, S. J., McMahon, A. P. and Tabin, C. J. (2007). Regulation of skeletogenic differentiation in cranial dermal bone. *Development* **134**, 3133-3144.
Ahn, D. and Ho, R. K. (2008). Tri-phasic expression of posterior Hox genes during development of pectoral fins in zebrafish: implications for the evolution of vertebrate paired appendages. *Dev. Biol.* **322**, 220-233.
Akimenko, M.-A., Marí-Beffa, M., Becerra, J. and Géraudie, J. (2003). Old questions, new tools, and some answers to the mystery of fin regeneration. *Dev. Dyn.* **226**, 190-201.
Ando, K., Shibata, E., Hans, S., Brand, M. and Kawakami, A. (2017). Osteoblast production by reserved progenitor cells in zebrafish bone regeneration and maintenance. *Dev. Cell* **43**, 643-650.e3.
Armstrong, B. E., Henner, A., Stewart, S. and Stankunas, K. (2017). Shh promotes direct interactions between epidermal cells and osteoblast progenitors to shape regenerated zebrafish bone. *Development* **144**, 1165-1176.
Askary, A., Mork, L., Paul, S., He, X., Izuhara, A. K., Gopalakrishnan, S., Ichida, J. K., McMahon, A. P., Dabizljevic, S., Dale, R. et al. (2015). Iroquois proteins promote skeletal joint formation by maintaining chondrocytes in an immature state. *Dev. Cell* **35**, 358-365.
Avaron, F., Hoffman, L., Guay, D. and Akimenko, M. A. (2006). Characterization of two new zebrafish members of the hedgehog family: atypical expression of a zebrafish indian hedgehog gene in skeletal elements of both endochondral and dermal origins. *Dev. Dyn.* **235**, 478-489.
Becerra, J., Junqueira, L. C. U., Bechara, I. J. and Montes, G. S. (1996). Regeneration of fin rays in teleosts: a histochemical, radioautographic, and ultrastructural study. *Arch. Histol. Cytol.* **59**, 15-35.
Borday, V., Thaëron, C., Avaron, F., Brulfert, A., Casane, D., Laurenti, P. and Géraudie, J. (2001). evx1 transcription in bony fin rays segment boundaries leads to a reiterated pattern during zebrafish fin development and regeneration. *Dev. Dyn.* **220**, 91-98.
Concordet, J. P., Lewis, K. E., Moore, J. W., Goodrich, L. V., Johnson, R. L., Scott, M. P. and Ingham, P. W. (1996). Spatial regulation of a zebrafish patched homologue reflects the roles of sonic hedgehog and protein kinase A in neural tube and somite patterning. *Development* **122**, 2835-2846.
Dardis, G., Tryon, R., Ton, Q., Johnson, S. L. and Iovine, M. K. (2017). Cx43 suppresses evx1 expression to regulate joint initiation in the regenerating fin. *Dev. Dyn.* **246**, 691-699.
Drissi, H., Zuscik, M., Rosier, R. and O'Keefe, R. (2005). Transcriptional regulation of chondrocyte maturation: potential involvement of transcription factors in OA pathogenesis. *Mol. Aspects Med.* **26**, 169-179.
Fromental-Ramain, C., Warot, X., Messadecq, N., LeMeur, M., Dollé, P. and Chambon, P. (1996). Hoxa-13 and Hoxd-13 play a crucial role in the patterning of the limb autopod. *Development* **122**, 2997-3011.
Gavaia, P. J., Simes, D. C., Ortiz-Delgado, J. B., Viegas, C. S. B., Pinto, J. P., Kelsh, R. N., Sarasquete, M. C. and Cancela, M. L. (2006). Osteocalcin and matrix Gla protein in zebrafish (Danio rerio) and Senegal sole (Solea senegalensis): comparative gene and protein expression during larval development through adulthood. *Gene Expr. Patterns* **6**, 637-652.
Goldsmith, M. I., Fisher, S., Waterman, R. and Johnson, S. L. (2003). Saltatory control of isometric growth in the zebrafish caudal fin is disrupted in long fin and rapunzel mutants. *Dev. Biol.* **259**, 303-317.
Hoptak-Solga, A. D., Nielsen, S., Jain, I., Thummel, R., Hyde, D. R. and Iovine, M. K. (2008). Connexin43 (GJA1) is required in the population of dividing cells during fin regeneration. *Dev. Biol.* **317**, 541-548.
Hulsey, C. D., Fraser, G. J. and Streelman, J. T. (2005). Evolution and development of complex biomechanical systems: 300 million years of fish jaws. *Zebrafish* **2**, 243-257.
Huycke, T. R., Eames, B. F. and Kimmel, C. B. (2012). Hedgehog-dependent proliferation drives modular growth during morphogenesis of a dermal bone. *Development* **139**, 2371-2380.
Iovine, M. K. and Johnson, S. L. (2000). Genetic analysis of isometric growth control mechanisms in the zebrafish caudal Fin. *Genetics* **155**, 1321-1329.
Iovine, M. K., Higgins, E. P., Hindes, A., Coblitz, B. and Johnson, S. L. (2005). Mutations in connexin43 (GJA1) perturb bone growth in zebrafish fins. *Dev. Biol.* **278**, 208-219.
Jeradi, S. and Hammerschmidt, M. (2016). Retinoic acid-induced premature osteoblast-to-preosteocyte transitioning has multiple effects on calvarial development. *Development* **143**, 1205-1216.
Johnson, S. L. and Bennett, P. (1998). Growth control in the ontogenetic and regenerating zebrafish fin. *Methods Cell Biol.* **59**, 301-311.
Johnson, S. L. and Weston, J. A. (1995). Temperature-sensitive mutations that cause stage-specific defects in zebrafish fin regeneration. *Genetics* **141**, 1583-1595.
Kherdjemil, Y., Lalonde, R. L., Sheth, R., Dumouchel, A., de Martino, G., Pineault, K. M., Wellik, D. M., Stadler, H. S., Akimenko, M.-A. and Kmita, M. (2016). Evolution of Hoxa11 regulation in vertebrates is linked to the pentadactyl state. *Nature* **539**, 89-92.
Klee, C. B. and Haiech, J. (1980). Concerted role of calmodulin and calcineurin in calcium regulation. *Ann. N. Y. Acad. Sci.* **356**, 43-54.
Knopf, F., Hammond, C., Chekuru, A., Kurth, T., Hans, S., Weber, C. W., Mahatma, G., Fisher, S., Brand, M., Schulte-Merker, S. et al. (2011). Bone regenerates via dedifferentiation of osteoblasts in the zebrafish fin. *Dev. Cell* **20**, 713-724.
Knosp, W. M., Scott, V., Bächinger, H. P. and Stadler, H. S. (2004). HOXA13 regulates the expression of bone morphogenetic proteins 2 and 7 to control distal limb morphogenesis. *Development* **131**, 4581-4592.
Kobayashi, T., Chung, U.-I., Schipani, E., Starbuck, M., Karsenty, G., Katagiri, T., Goad, D. L., Lanske, B. and Kronenberg, H. M. (2002). PTHrP and Indian hedgehog control differentiation of growth plate chondrocytes at multiple steps. *Development* **129**, 2977-2986.
Kronenberg, H. M. (2003). Developmental regulation of the growth plate. *Nature* **423**, 332-336.
Kujawski, S., Lin, W., Kitte, F., Börmel, M., Fuchs, S., Arulmozhivarman, G., Vogt, S., Theil, D., Zhang, Y. and Antos, C. L. (2014). Calcineurin regulates coordinated outgrowth of zebrafish regenerating fins. *Dev. Cell* **28**, 573-587.
Laforest, L., Brown, C. W., Poleo, G., Géraudie, J., Tada, M., Ekker, M. and Akimenko, M. A. (1998). Involvement of the sonic hedgehog, patched 1 and bmp2 genes in patterning of the zebrafish dermal fin rays. *Development* **125**, 4175-4184.
Lanske, B., Karaplis, A. C., Lee, K., Luz, A., Vortkamp, A., Pirro, A., Karperien, M., Defize, L. H. K., Ho, C., Mulligan, R. C. et al. (1996). PTH/PTHrP receptor in early development and Indian hedgehog-regulated bone growth. *Science* **273**, 663-666.
Lenton, K., James, A. W., Manu, A., Brugmann, S. A., Birker, D., Nelson, E. R., Leucht, P., Helms, J. A. and Longaker, M. T. (2011). Indian hedgehog positively regulates calvarial ossification and modulates bone morphogenetic protein signaling. *Genesis* **49**, 784-796.
Li, N., Felber, K., Elks, P., Croucher, P. and Roehl, H. H. (2009). Tracking gene expression during zebrafish osteoblast differentiation. *Dev. Dyn.* **238**, 459-466.
Long, F., Chung, U.-I., Ohba, S., McMahon, J., Kronenberg, H. M. and McMahon, A. P. (2004). Ihh signaling is directly required for the osteoblast lineage in the endochondral skeleton. *Development* **131**, 1309-1318.
Lotz, M., Hashimoto, S. and Kühn, K. (1999). Mechanisms of chondrocyte apoptosis. *Osteoarthritis Cartilage* **7**, 389-391.
Mari-Beffa, M., Mateos, I., Palmqvist, P. and Becerra, J. (1996). Cell to cell interactions during teleosts fin regeneration. *Int. J. Dev. Biol.* Suppl. 1, 179S-180S.
Nakashima, K., Zhou, X., Kunkel, G., Zhang, Z., Deng, J. M., Behringer, R. R. and de Crombrugghe, B. (2002). The novel zinc finger-containing transcription factor osterix is required for osteoblast differentiation and bone formation. *Cell* **108**, 17-29.
Nechiporuk, A. and Keating, M. T. (2002). A proliferation gradient between proximal and msxb-expressing distal blastema directs zebrafish fin regeneration. *Development* **129**, 2607-2617.
Padhi, B. K., Joly, L., Tellis, P., Smith, A., Nanjappa, P., Chevrette, M., Ekker, M. and Akimenko, M.-A. (2004). Screen for genes differentially expressed during regeneration of the zebrafish caudal fin. *Dev. Dyn.* **231**, 527-541.
Perathoner, S., Daane, J. M., Henrion, U., Seebohm, G., Higdon, C. W., Johnson, S. L., Nüsslein-Volhard, C. and Harris, M. P. (2014). Bioelectric signaling regulates size in zebrafish fins. *PLoS Genet.* **10**, e1004080.
Perez, W. D., Weller, C. R., Shou, S. and Stadler, H. S. (2010). Survival of Hoxa13 homozygous mutants reveals a novel role in digit patterning and appendicular skeletal development. *Dev. Dyn.* **239**, 446-457.

Poleo, G., Brown, C. W., Laforest, L. and Akimenko, M.-A. (2001). Cell proliferation and movement during early fin regeneration in zebrafish. *Dev. Dyn.* **221**, 380-390.
Poss, K. D., Keating, M. T. and Nechiporuk, A. (2003). Tales of regeneration in zebrafish. *Dev. Dyn.* **226**, 202-210.
Quint, E., Smith, A., Avaron, F., Laforest, L., Miles, J., Gaffield, W. and Akimenko, M.-A. (2002). Bone patterning is altered in the regenerating zebrafish caudal fin after ectopic expression of sonic hedgehog and bmp2b or exposure to cyclopamine. *Proc. Natl Acad. Sci. USA* **99**, 8713-8718.
Rolland-Lagan, A.-G., Paquette, M., Tweedle, V. and Akimenko, M.-A. (2012). Morphogen-based simulation model of ray growth and joint patterning during fin development and regeneration. *Development* **139**, 1188-1197.
Santamaría, J. A., Marí-Beffa, M., Santos-Ruiz, L. and Becerra, J. (1996). Incorporation of bromodeoxyuridine in regenerating fin tissue of the goldfish Carassius auratus. *J. Exp. Zool.* **275**, 300-307.
Santos-Ruiz, L., Santamaría, J. A., Ruiz-Sánchez, J. and Becerra, J. (2002). Cell proliferation during blastema formation in the regenerating teleost fin. *Dev. Dyn.* **223**, 262-272.
Schulte, C. J., Allen, C., England, S. J., Juárez-Morales, J. L. and Lewis, K. E. (2011). Evx1 is required for joint formation in zebrafish fin dermoskeleton. *Dev. Dyn.* **240**, 1240-1248.
Serra, R., Johnson, M., Filvaroff, E. H., LaBorde, J., Sheehan, D. M., Derynck, R. and Moses, H. L. (1997). Expression of a truncated, kinase-defective TGF-beta type II receptor in mouse skeletal tissue promotes terminal chondrocyte differentiation and osteoarthritis. *J. Cell Biol.* **139**, 541-552.
Serra, R., Karaplis, A. and Sohn, P. (1999). Parathyroid hormone-related peptide (PTHrP)-dependent and -independent effects of transforming growth factor beta (TGF-beta) on endochondral bone formation. *J. Cell Biol.* **145**, 783-794.
Sims, K., Jr, Eble, D. M. and Iovine, M. K. (2009). Connexin43 regulates joint location in zebrafish fins. *Dev. Biol.* **327**, 410-418.
Singh, S. P., Holdway, J. E. and Poss, K. D. (2012). Regeneration of amputated zebrafish fin rays from de novo osteoblasts. *Dev. Cell* **22**, 879-886.
Smith, A., Avaron, F., Guay, D., Padhi, B. K. and Akimenko, M. A. (2006). Inhibition of BMP signaling during zebrafish fin regeneration disrupts fin growth and scleroblast differentiation and function. *Dev. Biol.* **299**, 438-454.
Smith, A., Zhang, J., Guay, D., Quint, E., Johnson, A. and Akimenko, M. A. (2008). Gene expression analysis on sections of zebrafish regenerating fins reveals limitations in the whole-mount in situ hybridization method. *Dev. Dyn.* **237**, 417-425.
Sousa, S., Afonso, N., Bensimon-Brito, A., Fonseca, M., Simoes, M., Leon, J., Roehl, H., Cancela, M. L. and Jacinto, A. (2011). Differentiated skeletal cells contribute to blastema formation during zebrafish fin regeneration. *Development* **138**, 3897-3905.
St-Jacques, B., Hammerschmidt, M. and McMahon, A. P. (1999). Indian hedgehog signaling regulates proliferation and differentiation of chondrocytes and is essential for bone formation. *Genes Dev.* **13**, 2072-2086.
Stadler, H. S., Higgins, K. M. and Capecchi, M. R. (2001). Loss of Eph-receptor expression correlates with loss of cell adhesion and chondrogenic capacity in Hoxa13 mutant limbs. *Development* **128**, 4177-4188.
Thaëron, C., Avaron, F., Casane, D., Borday, V., Thisse, B., Thisse, C., Boulekbache, H. and Laurenti, P. (2000). Zebrafish evx1 is dynamically expressed during embryogenesis in subsets of interneurones, posterior gut and urogenital system. *Mech. Dev.* **99**, 167-172.
Thomas, J. L., Ochocinska, M. J., Hitchcock, P. F. and Thummel, R. (2012). Using the Tg(nrd:egfp)/albino zebrafish line to characterize in vivo expression of neurod. *PLoS ONE* **7**, e29128.
Ton, Q. V. and Iovine, M. K. (2013). Identification of an evx1-dependent joint-formation pathway during FIN regeneration. *PLoS ONE* **8**, e81240.
Tu, S. and Johnson, S. L. (2011). Fate restriction in the growing and regenerating zebrafish fin. *Dev. Cell* **20**, 725-732.
Vortkamp, A., Lee, K., Lanske, B., Segre, G. V., Kronenberg, H. M. and Tabin, C. J. (1996). Regulation of rate of cartilage differentiation by Indian hedgehog and PTH-related protein. *Science* **273**, 613-622.
Vortkamp, A., Pathi, S., Peretti, G. M., Caruso, E. M., Zaleske, D. J. and Tabin, C. J. (1998). Recapitulation of signals regulating embryonic bone formation during postnatal growth and in fracture repair. *Mech. Dev.* **71**, 65-76.
Welten, M. C. M., de Haan, S. B., van den Boogert, N., Noordermeer, J. N., Lamers, G. E. M., Spaink, H. P., Meijer, A. H. and Verbeek, F. J. (2006). ZebraFISH: fluorescent in situ hybridization protocol and three-dimensional imaging of gene expression patterns. *Zebrafish* **3**, 465-476.
Westerfield, M. (2007). *The Zebrafish Book: A Guide for the Laboratory Use of Zebrafish (Danio Rerio)*, 5th ed. University of Oregon Press: Eugene, OR.
Yan, Y.-L., Bhattacharya, P., He, X. J., Ponugoti, B., Marquardt, B., Layman, J., Grunloh, M., Postlethwait, J. H. and Rubin, D. A. (2012). Duplicated zebrafish co-orthologs of parathyroid hormone-related peptide (PTHrP, Pthlh) play different roles in craniofacial skeletogenesis. *J. Endocrinol.* **214**, 421-435.
Zhao, Q., Brauer, P. R., Xiao, L., McGuire, M. H. and Yee, J. A. (2002). Expression of parathyroid hormone-related peptide (PthrP) and its receptor (PTH1R) during the histogenesis of cartilage and bone in the chicken mandibular process. *J. Anat.* **201**, 137-151.

A Regulatory Pathway Involving Retinoic Acid and Calcineurin Demarcates and Maintains Joint Cells and Osteoblasts in the Fin Regenerate

Supplementary information

Table S1: Primers used for RT-PCR Analysis.

Primer Name	**Primer Sequence 5'-3'**
β-actin forward	ATGGATGAGGAAATCGCTGCCCTGGTC
β-actin reverse	CTCCCTGATGTCTGGGTCGTCCAAC
pthlha forward	CGTAATGCTGAGCCGGACA
pthlha reverse	TCACTGAACGCTTCATTCGGCT
pthlhb forward	AGCAGACAACGGCGTTCAGT
pthlhb reverse	GCATTTGGAAGGCACACGCT
pth1ra forward	TGTGCCAAATTCTTCCCCCA
pth1ra reverse	GAGCCGTCGAAAGTATCCGA

pth2R forward	CTTCTGTTCTCCGCGTCAGT
pth2R reverse	ATGCATGTGCTGCATGGTTG
pth1rb forward	AAGCATGGTGTCAGTGGAGG
pth1rb reverse	ACGCGTATCCTCTGTGGTTG

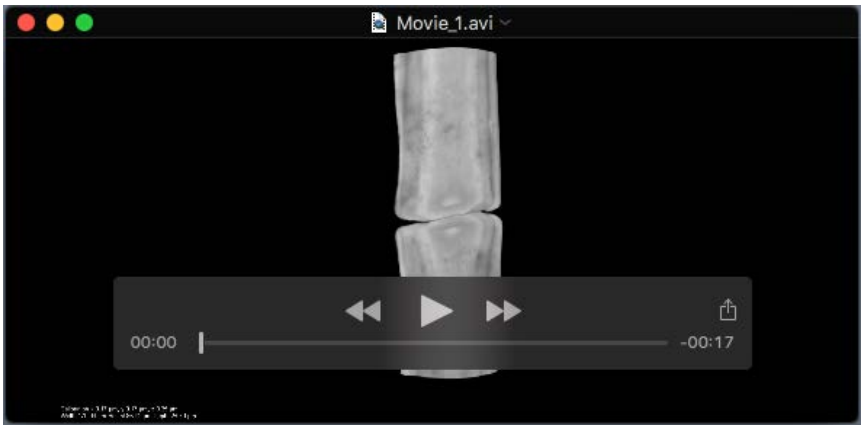

Movie 1: **Confocal 3D rendering of two fin ray segments.** 3D movie of Alizarin Red stained fin rays illustrates two consecutive segments in one hemiray that possess a concave shape.

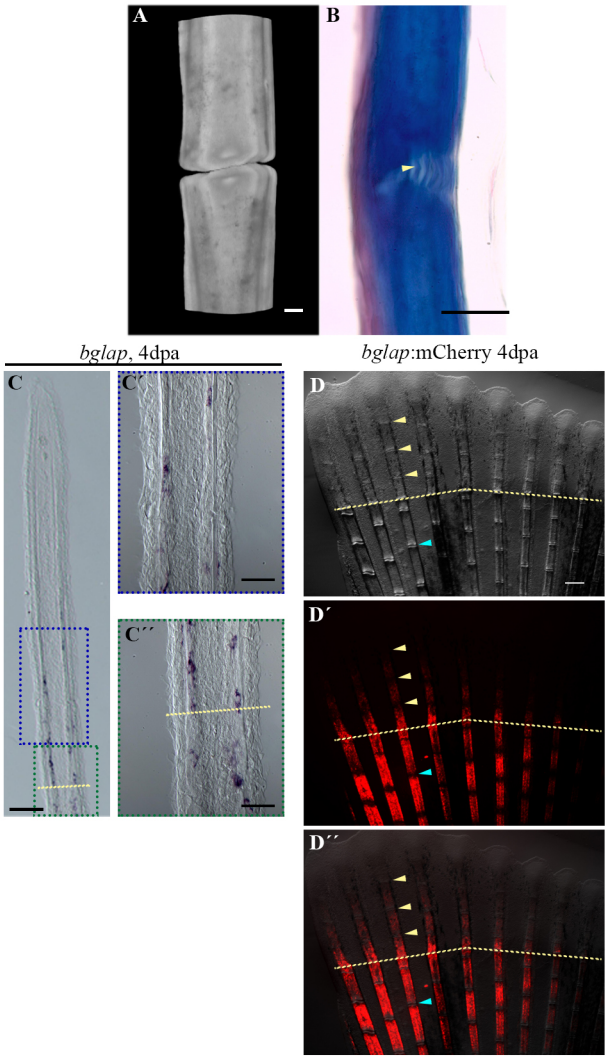

Supplementary figure 1

Fig. S1: Joint Structure. (A) Confocal 3D rendering of two fin ray segments separated by a joint. (B) Mallory staining illustrating two bone segments are connected by ligaments (yellow arrowhead). (C-C") ISH on longitudinal cryosections of 4dpa fin regenerates illustrate *bglap* expression in the proximal fin regenerate and stump osteoblasts. (C') Magnification of the proximal fin regenerate (blue box in C). (C") Magnification of the proximal fin regenerate and stump (green box in C). (D-D") *Tg(bglap:mCherry)* 4dpa regenerates illustrate mCherry expression in mature osteoblasts but not in joint regions in the fin regenerate (yellow arrowheads) and stump (blue arrowheads). (D) Brightfield only. (D') mCherry only. (D") merged. Amputation planes = dashed yellow line. Scale bars A=10µm, B=10µm, C=100µm, C'=50µm, C"=50µm, D-D''=200µm (shown in D).

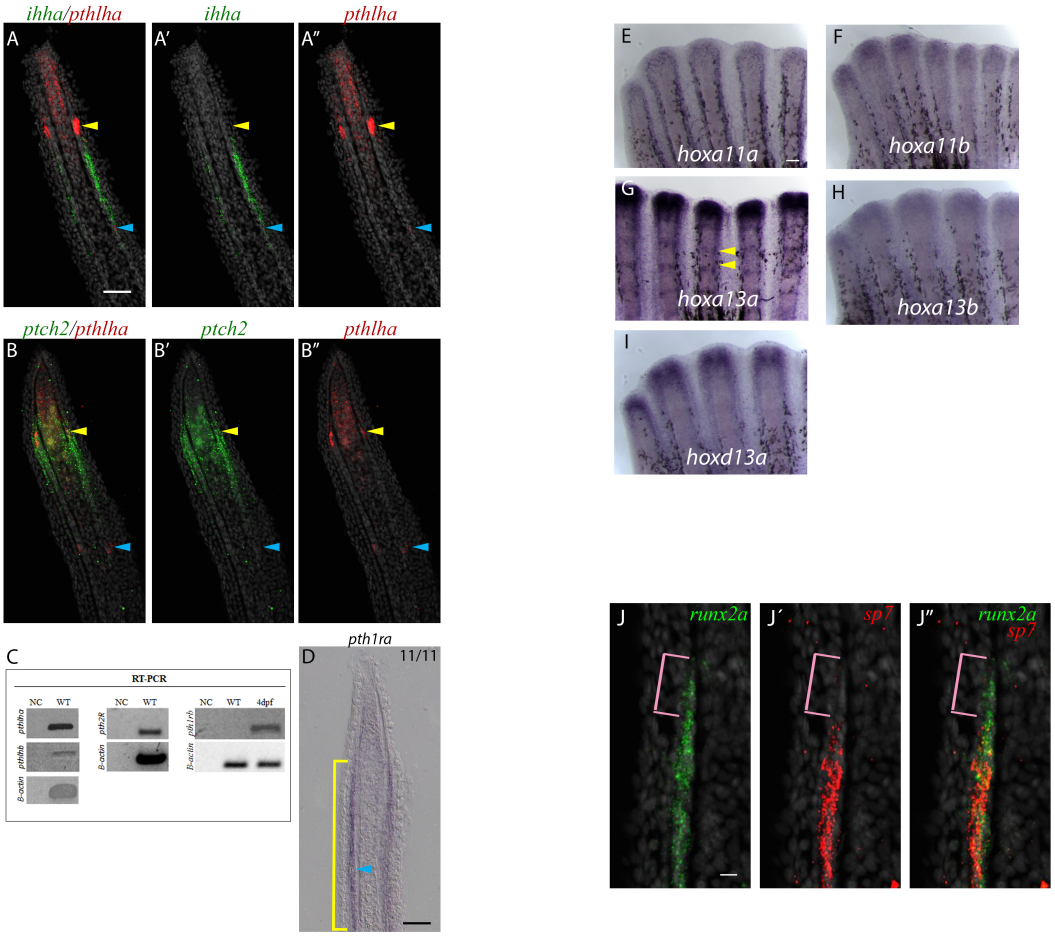

Supplementary figure 2

Fig. S2: Gene expression analysis of *hox* genes, *pthlha, ihha, pth1rb* and *ptch-2* at 4dpa. (A-A”) *pthlha* is expressed at the level of joints (blue and yellow arrowheads in A-A” and B-B”) while *ihha* is only found in osteoblasts (A-A”). (B-B”) *ptch2* is expressed in joint cells (yellow arrowheads) and differentiating osteoblasts, but not mature joints (blue arrowheads). (C) RT-PCR indicates *pthlha, pthlhb,* and *pth2r* are expressed in the 4dpa fin regenerates. *pth1rb* is not expressed in 4dpa wildtype fin regenerates, but is expressed in 4 days post fertilization (dpf) larvae. *β-actin* was used as the housekeeping control. NC = Negative Control. WT = wildtype. (D) In 11/11 sections, *pth1ra* is faintly expressed in differentiating osteoblasts (yellow bracket) and joint-forming cells (blue arrowhead). (E-I) ISH on whole mount fin regenerates indicate only *hoxa13a* is strongly expressed in joint regions (yellow arrowheads). Although faint staining appears in joints for *hoxa13b* (H) and *hoxd13a* (I), it is likely background as 4dpa fin regenerate sections do not show expression. (J-J”) Magnified images from Fig. 3D-D” to further illustrate the absence of *sp7* expression in the most distal *runx2a* expression domain (pink brackets). Scale bar A-B” = 50µm (shown in A), J-J’’=10µm (shown in J); D =50µm, E-I =100µm (shown in E).

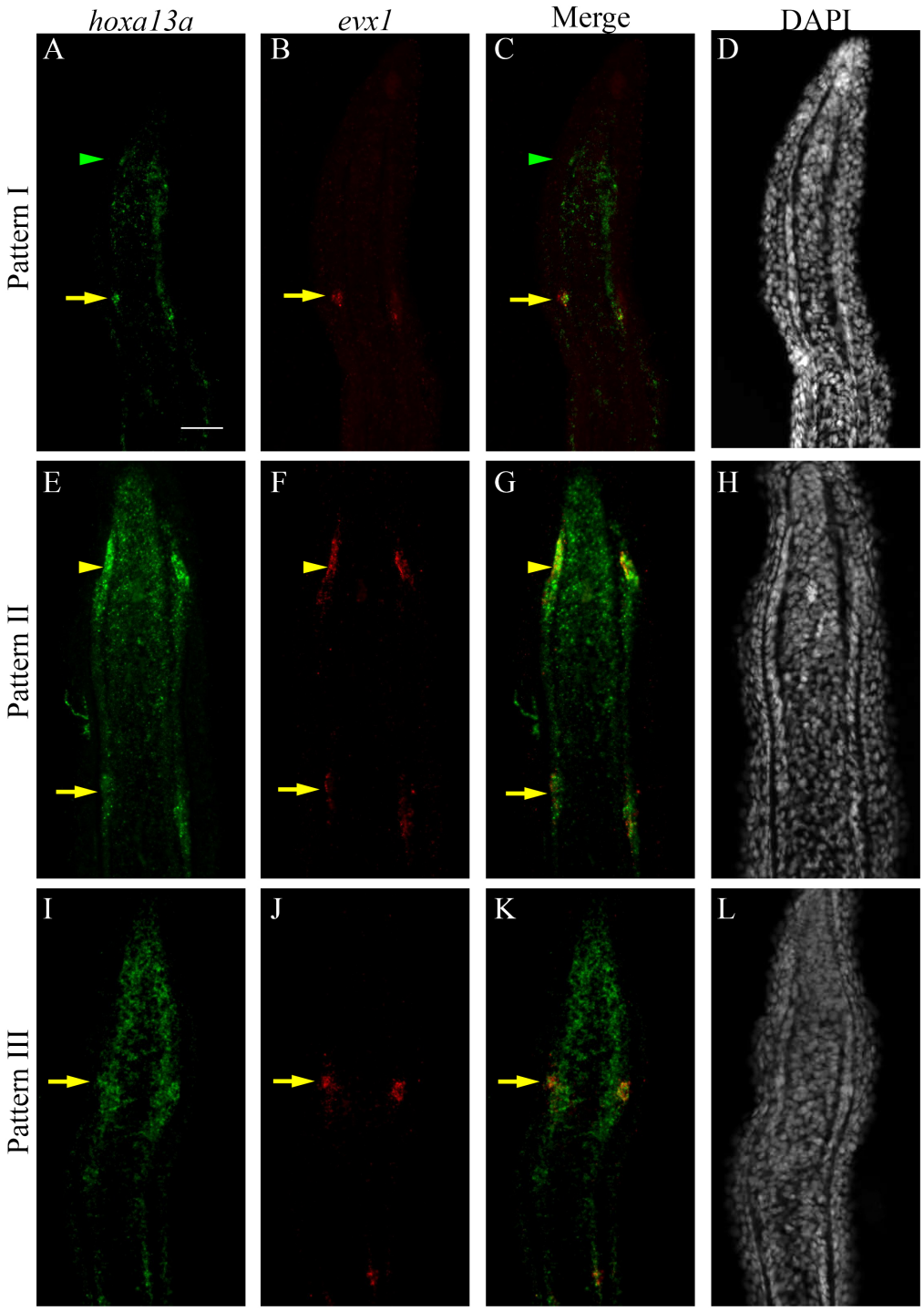

Supplementary figure 3

Fig. S3: Relative expression patterns of *hoxa13a* and *evx1*. (A-L) Double FISH (A-C, E-G, I-K) and DAPI counterstains (D, H, L) on longitudinal cryosections of 4dpa fin regenerates. (A-C, E-G, I-K) In joint-forming cells, *evx1* and *hoxa13a* are always co-expressed (yellow arrows). (A-H) In presumptive joint cells, *hoxa13a* is expressed either alone (Pattern I: A-D, green arrowheads) or is co-expressed with *evx1* (Pattern II: E-H, yellow arrowheads). (I-K) In Pattern III: *hoxa13a* and *evx1* are co-expressed in joint-forming cells when presumptive joint cells are not present (yellow arrows). (A, E, I) *hoxa13a* alone. (B, F, J) *evx1* alone. (C, G, K) *hoxa13a* and *evx1* expression merged. Scale Bars = 50μm (shown in A). These images are single image views for the merged images in Fig.4A-A".

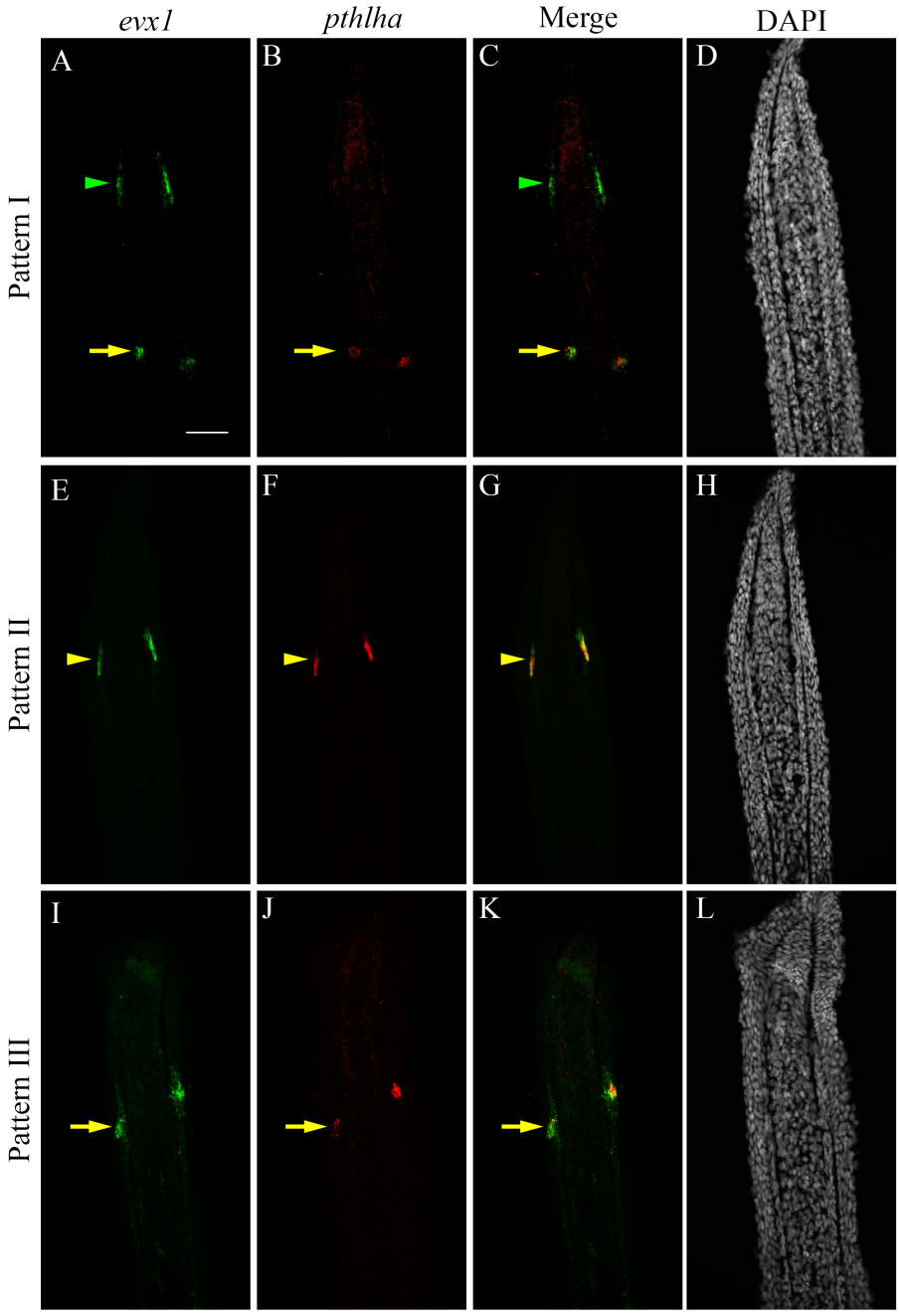

Supplementary figure 4

Fig. S4: Relative expression patterns of *evx1* and *pthlha*. (A-L) Double FISH (A-C, E-G, I-K) and DAPI counterstains (D, H, L) on longitudinal cryosections of 4dpa fin regenerates. (A-C, I-K) In joint-forming cells, *evx1* and *pthlha* are always co-expressed (yellow arrows). In presumptive joint cells, *evx1* is expressed either alone (Pattern I: A-D, green arrowheads) or is co-expressed with *pthlha* (Pattern II: E-H, yellow arrowheads). (I-L) In Pattern III: *evx1* and *pthlha* are expressed in joint-forming cells when presumptive cells are not yet present (yellow arrows). (A, E, I) *evx1* expression alone. (B, F, J) *pthlha* expression alone. (C, G, K) *evx1* and *pthlha* expression merged images. Scale Bars = 50μm (shown in A). These images are single image views for the merged images in Fig.4B-B".

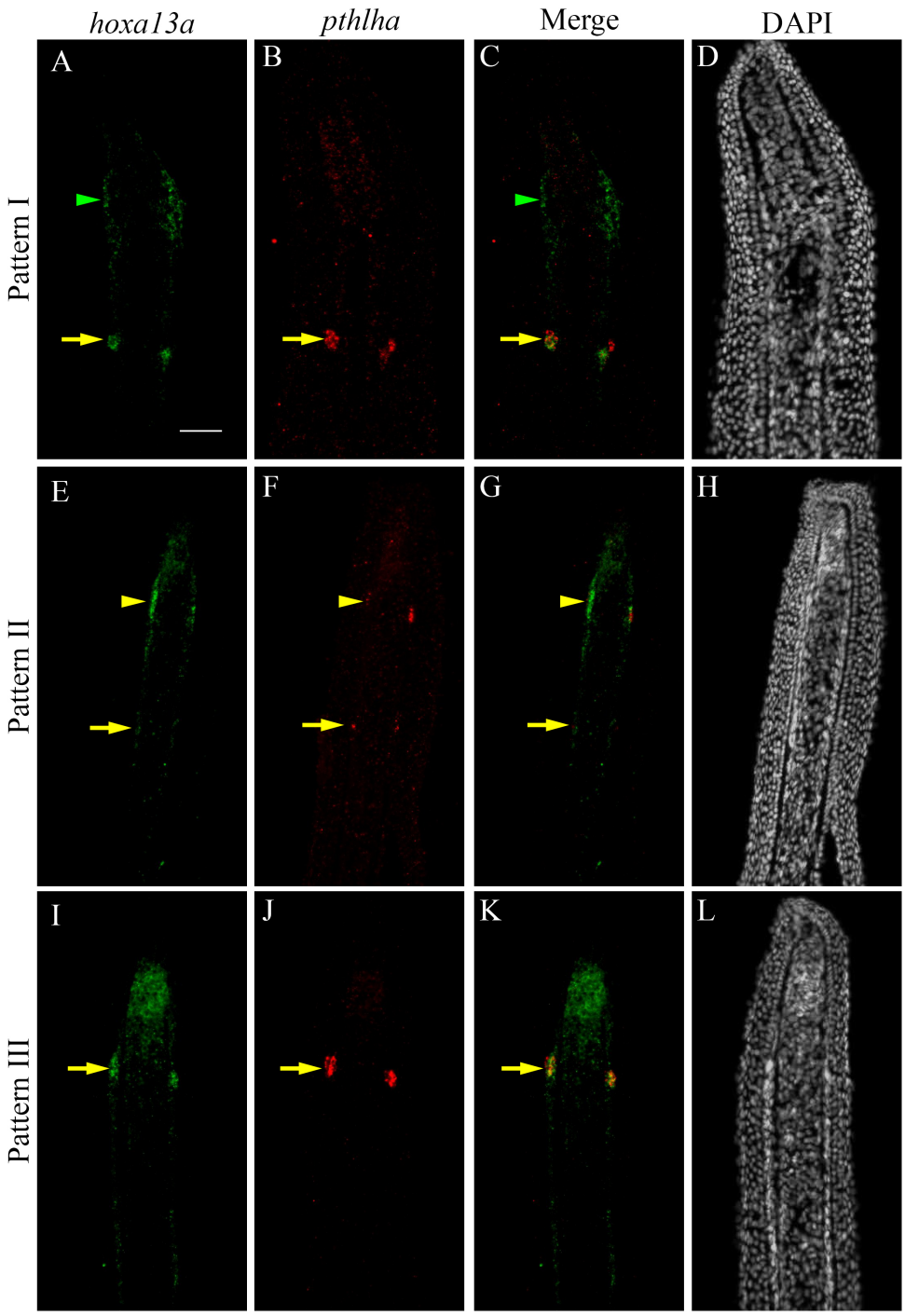

Supplementary figure 5

Fig. S5: Relative expression patterns of *hoxa13a* and *pthlha*. (A-L) Double FISH (A-C, E-G, I-K) and DAPI counterstains (D, H, L) on longitudinal cryosections of 4 dpa fin regenerates. (A-C, E-G, I-K) In joint-forming cells, *hoxa13a* and *pthlha* are always co-expressed (yellow arrows). In presumptive joint cells, *hoxa13a* is expressed either alone (Pattern I: A-D, green arrowheads) or is co-expressed with *pthlha* (Pattern II: E-H, yellow arrowheads). (I-L) In Pattern III: *hoxa13a* and *pthlha* are expressed in joint-forming cells when presumptive cells are not yet present (yellow arrows). (A, E, I) *hoxa13a* expression alone. (B, F, J) *pthlha* expression alone. (C, G, K) *hoxa13a* and *pthlha* expression merged. Scale Bars = 50μm (shown in A). These images are single image views for the merged images in Fig.4C-C".

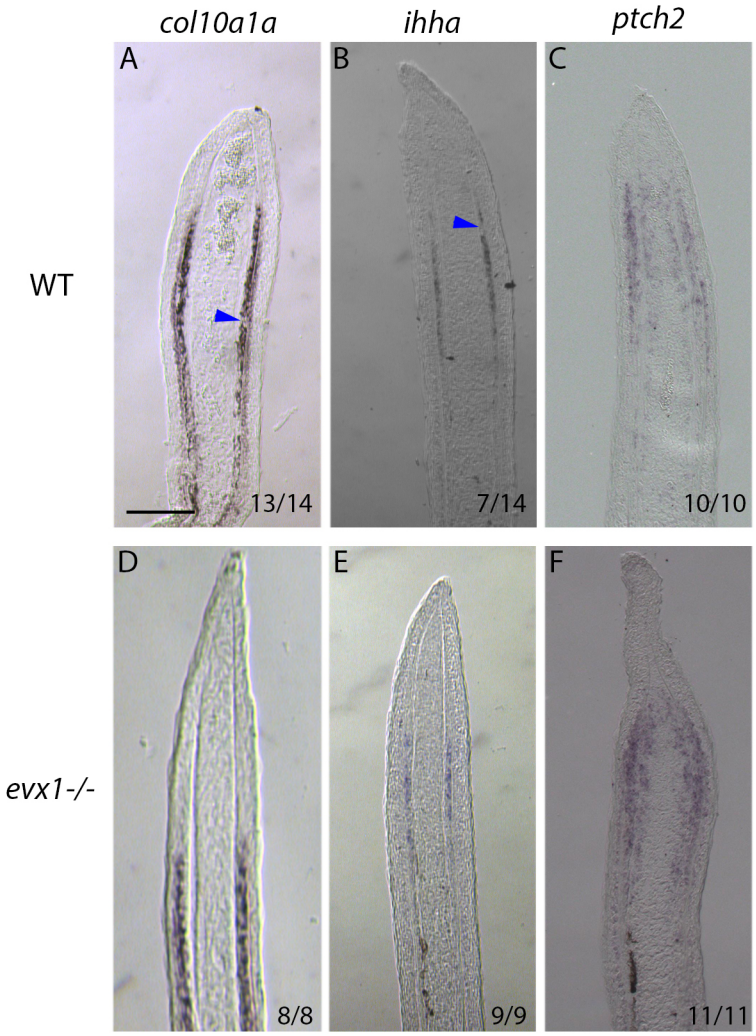

Supplementary figure 6

Fig. S6: Gene expression analyses in wildtype and *evx1*$^{-/-}$ loss of function mutants. In wildtype longitudinal cryosections *col10a1a* (A) and *ihha* (B) are expressed in osteoblasts with gaps corresponding to joint cells (blue arrowheads). There is no change in *ptch2* expression between wildtype (C) and *evx1*$^{-/-}$ mutants (F). However, in *evx1*$^{-/-}$ mutants, *col10a1a* (D) and *ihha* (E) are expressed in a continuous pattern without the gaps corresponding to the position of joints. Scale bars for all panels = 100µm (shown in A). Numbers in each panel represent the number of sections with the expression pattern over the total number of sections analyzed.

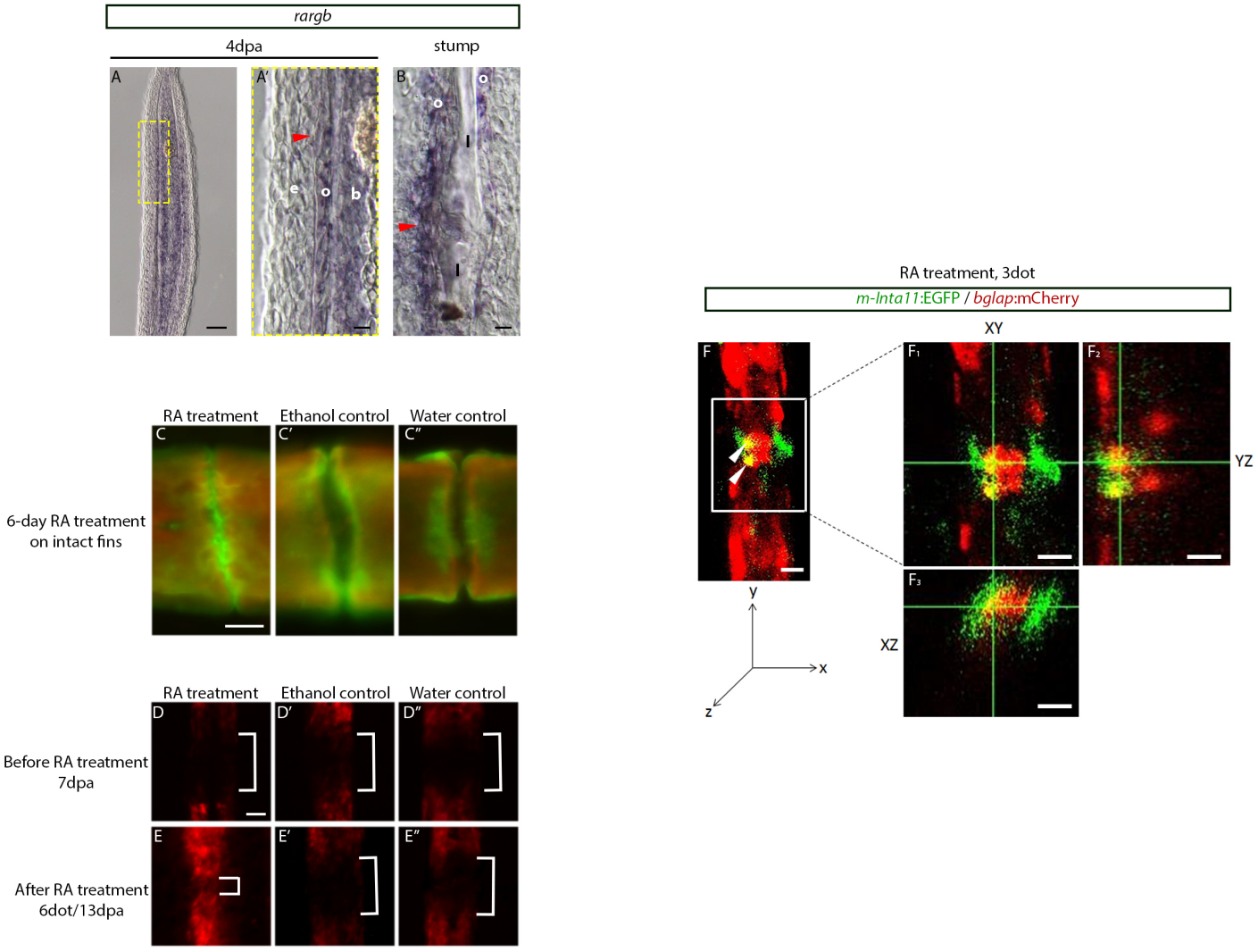

Supplementary figure 7

Fig. S7: Retinoic Acid Treatment leads to bone deposition and osteoblast encroachment in joint regions. (A) ISH on 4dpa fin regenerates indicating *rargb* is expressed in osteoblasts and blastema of the 4dpa fin regenerate. (A') Magnified image from the yellow box in A indicating *rargb* is expressed in osteoblasts, blastema, and joint-forming cells (red arrowhead). (B) *rargb* is also expressed in mature joint cells (red arrowhead) surrounding the lepidotrichia. (C) Calcein (green) and alizarin red (red) stains illustrate that 6dot with RA results in new bone deposition (green) in joints of intact fins when compared to ethanol (C') and water (C") controls. (D-D") Prior to RA treatment, *Tg(bglap:mCherry)* fin regenerates do not possess mCherry expressing osteoblasts in joint regions (white brackets). (E) 13dpa/6dot with RA: mCherry-expressing osteoblasts are observed in the joints (white bracket). No mCherry-expressing osteoblasts are in joint regions in ethanol (E', D') and water (E", D") controls (white brackets). (F) Confocal image of *Tg(m-Inta11:EGFP; bglap:mCherry)* following 3 dot with RA. Image of the XY (F_1), YZ (F_2), and XZ (F_3) planes illustrating a joint cell co-expressing EGFP and mCherry (yellow). osteoblasts (o), blastema (b), lepidotrichia (l), basal epidermis (e). Scale Bars: A=50μm; A'-B=10μm; C-C''=10μm (shown in C); D-E''=50μm (shown in D); F-F_3=20μm.